Design of a Modified Cherry-Hooper Transimpedance Amplifier with DC Offset Cancellation

by

Kyle LaFevre

A Thesis Presented in Partial Fulfillment
of the Requirements for the Degree
Master of Science

Approved July 2011 by the
Graduate Supervisory Committee:

Bertan Bakkaloglu, Chair
Bert Vermeire
Hugh Barnaby

ARIZONA STATE UNIVERSITY

August 2011

ABSTRACT

Optical receivers have many different uses covering simple infrared receivers, high speed fiber optic communication and light based instrumentation. All of them have an optical receiver that converts photons to current followed by a transimpedance amplifier to convert the current to a useful voltage. Different systems create different requirements for each receiver. High speed digital communication require high throughput with enough sensitivity to keep the bit error rate low. Instrumentation receivers have a lower bandwidth, but higher gain and sensitivity requirements.

In this thesis an optical receiver for use in instrumentation in presented. It is an entirely monolithic design with the photodiodes on the same substrate as the CMOS circuitry. This allows for it to be built into a focal-plane array, but it places some restriction on the area. It is also designed for in-situ testing and must be able to cancel any low frequency noise caused by ambient light. The area restrictions prohibit the use of a DC blocking capacitor to reject the low frequency noise. In place a servo loop was wrapped around the system to reject any DC offset.

A modified Cherry-Hooper architecture was used for the transimpedance amplifier. This provides the flexibility to create an amplifier with high gain and wide bandwidth that is independent of the input capacitance. The downside is the increased complexity of the design makes stability paramount to the design. Another drawback is the high noise associated with low input impedance that decouples the input capacitance from the bandwidth. This problem is

compounded by the servo loop feed which leaves the output noise of some amplifiers directly referred to the input. An in depth analysis of each circuit block's noise contribution is presented.

Dedicated to my family.

ACKNOWLEDGMENTS

I would like to thank my advisor Dr. Bertan Bakkaloglu for his support throughout this project. He has been an inspiration for me to attain the breadth of knowledge he posses' and share it in the same jovial manner he does. I would also like to thank Dr. Bert Vermaire for his support and ability to shield me from the mess of acquiring funding for this work. Dr. Hugh Barnaby was also tremendously helpful with this work. I want to thank him for answering any question I brought to him and coordinating my work with some of my peers.

I would also like to thank my family for always supporting me while I have pursued my education. I am particularly thankful for my wonderful wife who agreed to follow me into the desert while I pursue a higher education.

TABLE OF CONTENTS

CHAPTER 4: SIMULATION RESULTS Page

LIST OF FIGURES

Figure		Page

LIST OF TABLES

PREFACE

The design of an optical receiver, like most electronics design, is full of tradeoffs. This study delves into the design of a monolithic photodiode and transimpedance amplifier for use in an instrumentation system such as a laser vibrometer. For the transimpedance amplifier a modified Cherry-Hooper topology was used. One of the primary challenges for this type of receiver is low frequency noise caused by ambient light and the laser itself. A servo loop was implemented to cancel out any low frequency noise or DC input offset.

Chapter 1 introduces the concept of a transimpedance amplifier. An explanation of why this circuit is useful is shown along with some critical design parameters.

Chapter 2 covers conventional TIA design. An analysis of the different stages used in the presented Cherry-Hooper design was made. The advantages and drawbacks of the different design are highlighted with a focus on low noise design.

Chapter 3 describes how the servo loop cancels any input DC offset while providing the design details of the entire system. The transistor level design and bias conditions for each stage is provided with an explanation of how each portion impacts the entire design.

Chapter 4 presents the simulation results for the entire design. A juxtaposition of predicted performance and simulated results is provided. The device was manufactured, but budget and time constraints prohibited the results from being available for this paper. The characterization will be included with the following doctoral dissertation.

CHAPTER 1 INTRODUCTION

1.1 TIA USES AND OVERVIEW

Optical receivers are a common occurrence in everyday life. They may be a small part of a system, like the infrared receiver on a television, or a very complex system as part of a modern high speed fiber optic communication scheme. What every receiver has in common is they all use a photodiode to convert photons to current and a transimpedance amplifier to convert the current to a useful output voltage. This paper is focused on a monolithic optical receiver for use in a laser vibrometer system.

Many different laser vibrometers already exist, but they all large and only suited for use inside of a laboratory. Creating an optical receiver specifically for a laser vibrometer is a step to allow the entire system to be miniaturized and made portable. As shown in (14) a scanning laser vibrometer system is very useful for shallow underground imaging. Ground penetrating radar has been extensively used for underground imaging, but has many drawbacks a laser vibrometer system can address. The most important improvements with the laser vibrometer are its ability to detect nonmetal objects, work in any soil type and detect objects that are less than 30cm deep.

Designing an optical receiver for a laser vibrometer provides some unique challenges. A very high resolution ADC will be used so the noise of the system must be less than an LSB of the ADC. Also the amplifier will be used *in-situ* and so it must be able to ignore any unwanted signals. These unwanted signals include ambient light, noise from the laser source and anything else.

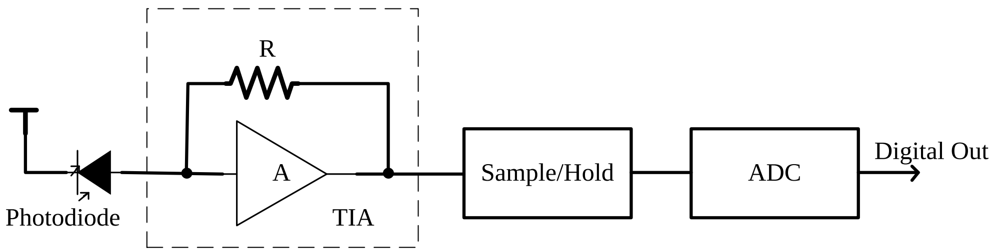

Fig. 1 A block diagram of a general photodiode receiver circuit

The focus of this paper is the transimpedance amplifier. Current research in TIA design is focused on high speed digital communication. These receivers typically have less gain with a wider bandwidth. They are often single ended receivers employing inductive peaking to try and get the bandwidth as wide as possible with current technology. Often, they are characterized using eye diagrams and bit error rate. The amplifier proposed here is a high gain, lower bandwidth design for analog purposes. Linearity over a range of frequencies is important so the amplifier is characterized by its gain, bandwidth, input referred noise, and harmonic distortion.

The TIA was implemented using a Cherry-Hooper topology. This topology has a low input impedance which allows for a large photodiode with a large parasitic capacitance, but it would also requires the input to be DC coupled since a DC blocking capacitor has to be very large. The gain and bandwidth are also independently tunable to achieve a high gain with a wide bandwidth. The drawbacks to this design is the output dynamic range is limited and the input is DC coupled.

Since the design must be DC coupled any input offset has to potential to saturate the amplifier. A servo loop was used to keep the amplifier from saturating by cancelling out any input offset. The design is required to cancel out a DC offset that is up to ten times larger than the signal of interest. The servo loop works by shunting any DC or low frequency current to ground to keep it from entering the amplifier.

1.2 THESIS STRUCTURE

CHAPTER 2 describes the different methods of characterizing a TIA, how they are measured and what they mean. A block by block analysis of the system is then described, with each blocks characterization and implications of those measurements on the system. CHAPTER 3 covers the actual design that was manufactured and all of the simulation results are also presented. CHAPTER 4 concludes this paper with the test plan, measurement setup and measurement results.

CHAPTER 2 CONVENTIONAL TIA DESIGN

2.1 OPTICAL RECEIVER BASICS

The basis of an optical receiver is the photodiode and significant research is going in to making them more useful in optical receivers. A photodiode works by converting an incident optical signal into an electrical current. It is a square law device where the electrical current depends on the power of the incident optical signal. The TIA typically has a linear output voltage that is followed by either a high gain limiting amplifier (LA) or analog to digital converter (ADC) depending how the signal is to be used.

High gain LAs are used to convert the relatively small signal TIA output to a full scale rail-to-rail output voltage. The LA is a non-linear amplifier with an output that saturates for very small input signals. The use of this is to generate an output voltage that is constant over a range of input voltages. This output voltage is also large enough to be considered a detectable logic level. This can then be used with a flip-flop and clock recovery circuit to act as a digital receiver.

The focus of this thesis is on the TIA which is commonly referred to as the analog front end (AFE) of any optical receiver circuit. This circuit was designed to be followed by analog filters and an ADC which makes the specifications very different from a digital receiver. It is a very high gain amplifier design to sense a high frequency small signal that is riding on top of a low frequency signal whose variation is 10 times greater than the desired signal. Such a large DC input variation would saturate the amplifier without DC input compensation. A servo loop was wrapped around the amplifier which shunts any low frequency noise to ground while allowing the higher frequency signal to pass into the amplifier.

2.1.1 RECEIVER SPECIFICATIONS

Digital optical receivers are characterized by sensitivity and achievable bit rate. Sensitivity is measured as bit error rate (BER). BER is defined as the number of incorrectly detected bits per total number of bits sent and is typically on the order of 10^{-12}. BER is very useful figure of merit since it depends on the gain, bandwidth, and input referred noise of the amplifier. In a design the required BER and achievable bit rate entirely define the requirements of the TIA.

For the analog receiver presented here the specifications are different. Noise requirements are much greater for the analog design while gain and bandwidth are directly specified. A unique specification to the design is the amount of dark current it can handle. Dark current is the output current of the photodiode from ambient light and low frequency noise. The following table shows the required design specifications. The primary challenges are the low input referred noise specification and the ability to reject dark current that is 10 times greater than the input signal level.

Table 1: Design specifications for TIA.

Parameter	**Specification**
Transimpedance Gain (Z_T)	210kΩ
Input Impedance (C_{PD})	0.8pF

Input Dynamic Range	4nA to 4μA
Output Dynamic Range	1mV to 1V
Input Referred Noise Density	$0.35pA/\sqrt{Hz}$
Bandwidth	15MHz to 35MHz
Gain Bandwidth Product	6.3THz*Ω
Dark Current	0 to 40μA

2.2 BASICS OF A TRANSIMPEDANCE AMPLIFIER

The purpose of a transimpedance amplifier is to convert the output current of a photodiode to a useful voltage. The ratio of the output voltage to in the input current is the transimpedance gain of the amplifier

$$Z_T = \left|\frac{V_{out}}{I_{in}}\right| \tag{2.21}$$

Noise of TIA is defined by the input referred noise. Input referred noise is the current noise that would be added to an equivalent noiseless TIA. Noise measurement is made by observing the output noise voltage and dividing it down by the transimpedance gain. Figure 2.1 shows the equivalent noise circuits defined in equation 2.22

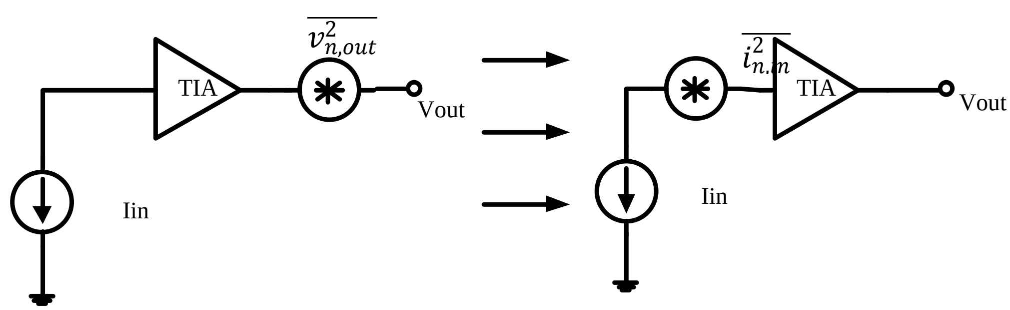

Fig. 2: Input referred noise.

$$\overline{|i_{n,in}|^2} = \frac{\overline{|v_{n,out}|^2}}{|Z_T|^2} \tag{2.22}$$

2.3 PRIMITIVE TRANSIMPEDANCE AMPLIFIER

The most basic way to create a TIA is to simply use a resistor. This is shown in figure 3. The current to voltage transformation is well known by Ohm's law. The downside to such a simple receiver is the gain, bandwidth, and noise are dependent on the resistance.

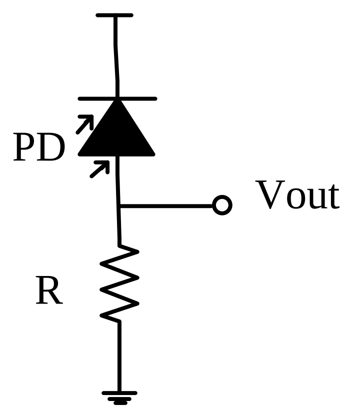

Fig. 3: Photodiode with load resistance.

The transimpedance gain R_T is simply equal to R_L. The –3dB bandwidth is simply the RC time constant formed by the load and the parasitic capacitance of the photodiode, C_{PD}. This implies that increasing the bandwidth of the TIA requires a reduced gain.

$$f_{-3dB} = \frac{1}{2\pi R_L C_{PD}} \tag{2.31}$$

The noise of the system is also set by R_L. A schematic with noise sources is shown in figure 4. Since the thermal noise of the resistor is in parallel with the input current, all of the noise shows up at the input so the input referred noise is equal to the resistor noise. Equation 2.32 shows the input referred noise with k_B being Boltzmann's constant and T is temperature in Kelvin.

$$\overline{i_{n,in}^2} = \frac{4k_B T}{R_L} \qquad (2.32)$$

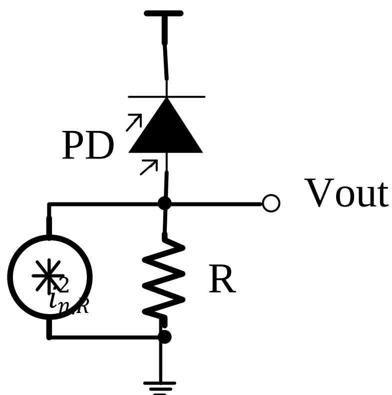

Fig. 4: Photodiode and resistor with noise sources.

A more complex design is required in order to decouple the gain, bandwidth and noise. These circuits allow for the gain and bandwidth to be independent of the parasitic input capacitance. They also allow for a greater dynamic range.

2.4 SHUNT-SHUNT TRANSIMPEDANCE AMPLIFLIER

One of the more common TIA topologies is the shunt-shunt amplifier. It is made up of a voltage amplifier with a shunt feedback resistor as shown in figure 5. The high input impedance of the voltage amp forces all of the input current through the feedback resistor. This causes the gain of the TIA to be equal to the feedback resistance assuming the gain of the voltage amplifier is much greater than one.

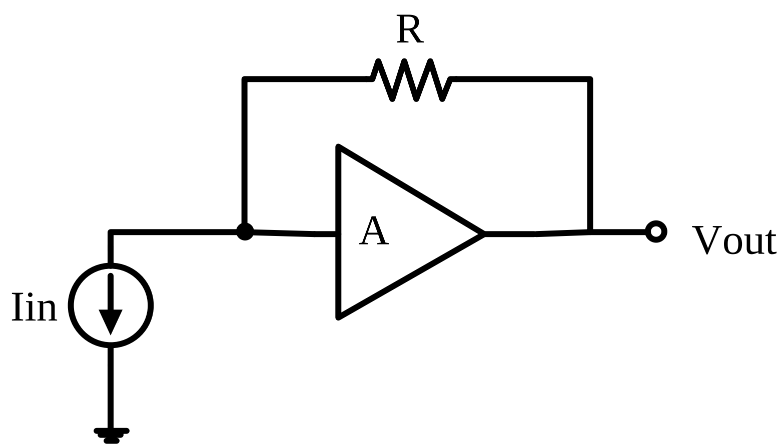

Fig. 5 Model of transresistance amplifier

$$Z_T = \frac{R_f * A_0}{A_0 + 1} \tag{2.41}$$

$$If A_0 \gg 1 \text{ then}$$

$$Z_T = R_f \tag{2.42}$$

While it initially appears that this amplifier is the same as the primitive the difference can be seen in the frequency response. The dominant pole of the system is increased by a factor equal to the gain of the amplifier. This is from the amplifier making the effective input resistance seen by the photodiode equal to the feedback resistance divided down by the amplifier gain. Assuming $R_{out} << R_f$ the following poles are observed

$$f_1 = \frac{A_0}{2\pi R_f C_{pd}} \tag{2.43}$$

$$f_2 = \frac{1}{2\pi R_{OUT} C_L} \tag{2.44}$$

This amplifier is often treated as a single pole system with f_1 the dominant pole, but if f_1 and f_2 are close it must be viewed as a 2nd order system with the following definition

$$\left({}^{s}/_{\omega_n}\right)^2 + 2Q\left({}^{s}/_{\omega_n}\right) + 1 = 0 \tag{2.45}$$

$$Where$$

$$\omega_n = \sqrt{\frac{A_0 + 1}{R_f R_{out} C_{pd} C_L}} \tag{2.46}$$

$$Q = \frac{1}{2} \frac{\frac{R_f C_{pd}}{R_{out} C_L} + 1}{\sqrt{(A_0 + 1)\frac{R_f C_{pd}}{R_{out} C_L}}} \tag{2.47}$$

With the second order system value of Q must be large for the amplifier to remain stable. It is possible to achieve a very wide bandwidth and high gain with a very low Q, but it is unrealistic to expect the amplifier to work. As Q decreases the phase margin also decreases with a larger amount of ringing and overshoot. A generally accepted compromise is to set Q equal to 0.7 to provide a good tradeoff between ringing and stability.

2.5 COMMON GATE TRANSIMPEDANCE AMPLIFIER

A common gate or base topology is typically used for the input stage of a TIA since it provides low input impedance. The low input impedance allows for a large parasitic capacitance of the photodiode without limiting the bandwidth of the TIA. Figure 6 shows a common gate schematic.

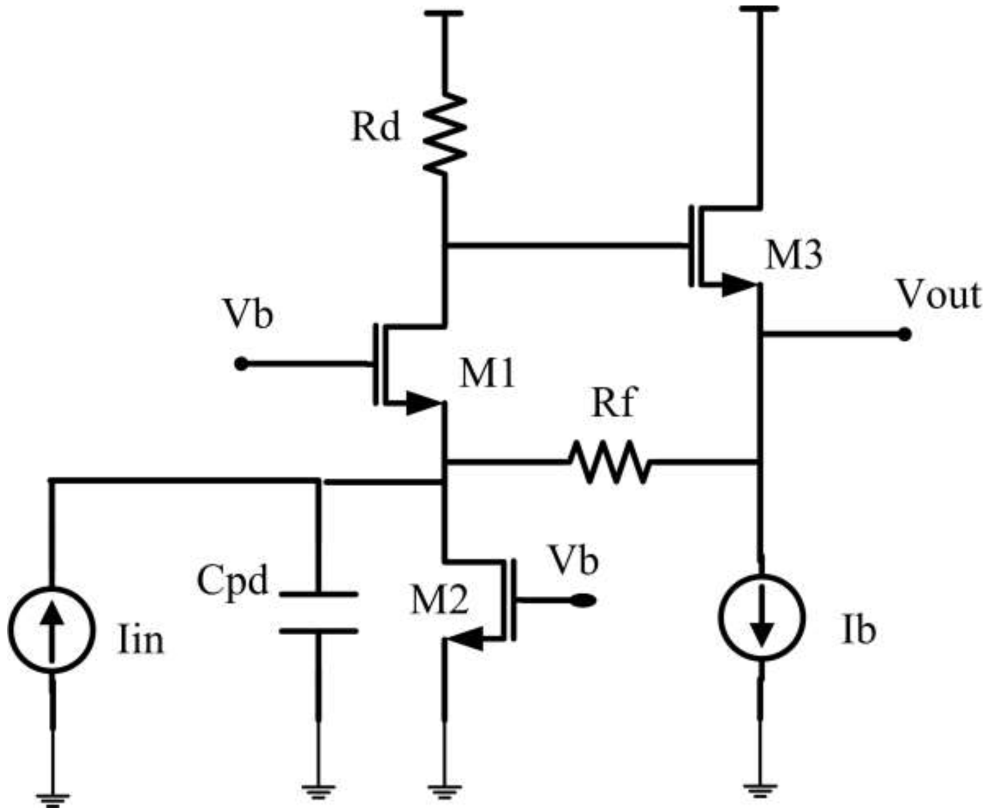

Fig. 6: Common gate architecture.

In this configuration M1 is the common gate transistor while M2 acts as the current source to bias the circuit. All of the input current is mirrored over and passed to R_f which gives the amplifier a gain equal to the value of R_f. The input impedance is shown in equation 2.51.

$$R_{in} = {}^{1}\!/_{g_{m1}} || r_{ds2} || \left(R_f + {}^{1}\!/_{g_{m3}}\right) \tag{2.51}$$

It is then safe to assume that $1/g_{m1}$ is much less than r_{ds2} which makes the input impedance equal to the transconductance of the common gate transistor.

$$R_{in} = {}^{1}\!/_{g_{m1}} \tag{2.52}$$

The output impedance of the amplifier is the parallel combination of R_d and the output impedance of the M1 and M2 cascode. This simplifies down to the equation shown in 2.53.

$$R_o = R_d \tag{2.53}$$

This implies that the dominant pole of the amplifier will be at the output with a time constant of R_o*C_L. The advantage is that the parasitic capacitance of the photodiode no longer defines the bandwidth of the amplifier. Since the parasitics of the photodiode can be very large this design usually has a wider bandwidth than the previous topologies.

The primary drawback to this configuration is the input referred noise of the circuit. In the previous designs the dominant noise source is the feedback resistor R_f while the noise of the common gate design is primarily from the input device. Since the purpose of the common gate design is to have a low input impedance the input device must have a large g_m which means its noise contribution is also large. The current noise density is shown in equations 2.54 and 2.55 where γ is a factor of transistor parameters and bias conditions that must be numerically solved.

$$\overline{i_n^2} = \gamma k_B T g_m \tag{2.46}$$

$$\overline{i_n^2} = \frac{4k_B T}{R} \tag{2.47}$$

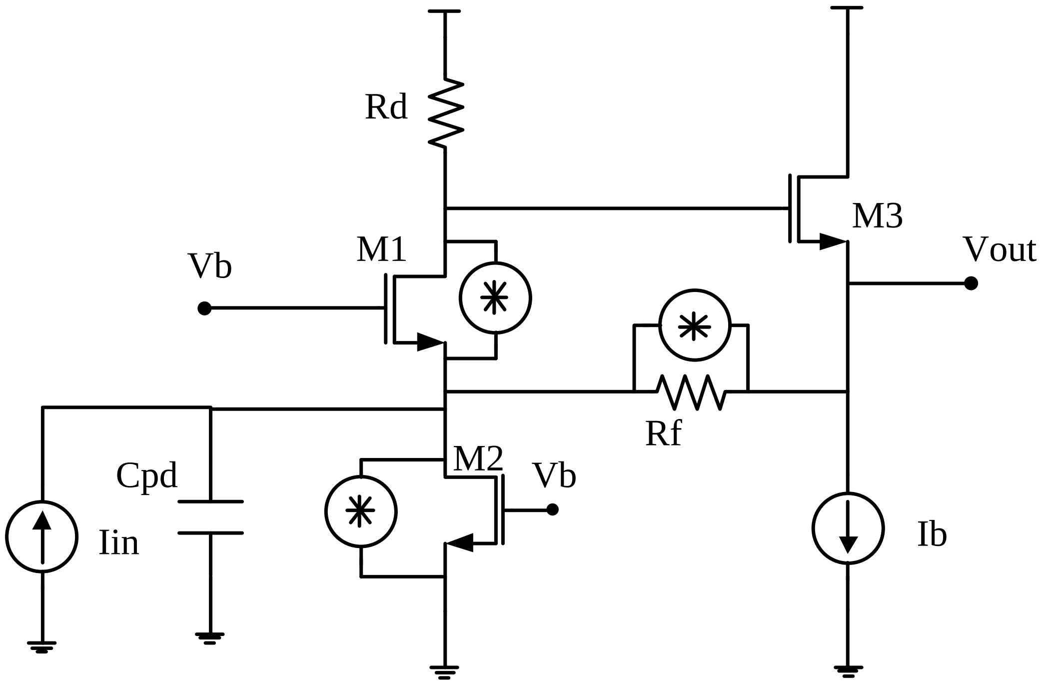

Fig. 7: Common gate amplifier with major noise sources shown.

2.6 REGULATED GATE CASCODE

A common improvement to the common gate amplifier is the regulated gate cascode. A voltage amplifier is added from the source to gate of the input transistor. This amplifier works to increase the transconductance of the input transistor which lowers the input impedance by a factor equal to the gain of the voltage amplifier. The lower the input impedance the less impact the photodiode's parasitic capacitance has on the frequency response of the circuit. These circuits are used with large and sensitive diodes.

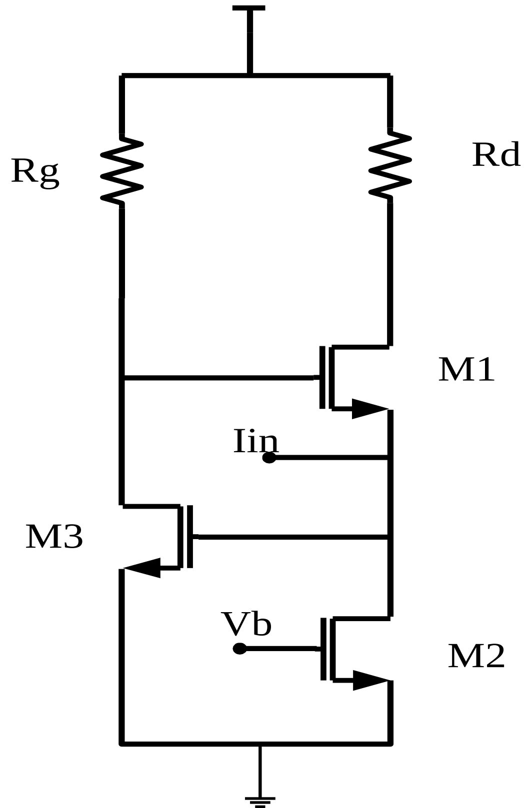

Fig. 8: Input of regulated gate cascode amplifier.

Figure 8 shows a CMOS implementation of the input stage of a regulated gate cascode amplifier. The voltage amplifier is a common source topology using M3 as the input and R_g as the load impedance. The input impedance is shown in equation 2.61.

$$R_{in} = \frac{1}{g_{m1}(1 + g_{m3}R_g)} \tag{2.61}$$

Aside from the reduced input impedance the amplifier has the similar performance as the common gate architecture. The lower R_{in} is a result of the effective g_m of the input device being higher. From looking at equation 2.46 it can be seen that increasing the input devices transconductance has the adverse effect of increasing the input referred noise, but with a large input capacitance this circuit becomes the only option.

2.7 CHERRY-HOOPER DESIGN

The Cherry-Hooper topology was devised to allow the gain and bandwidth of an amplifier to be tuned independently of each other. Figure 2.7 shows the basic premise of the circuit. It is composed of two g_m stages, the first input stage which converts the input signal to a current and the second stage with a shunt feedback resistor to convert the current (i_x) into the output voltage.

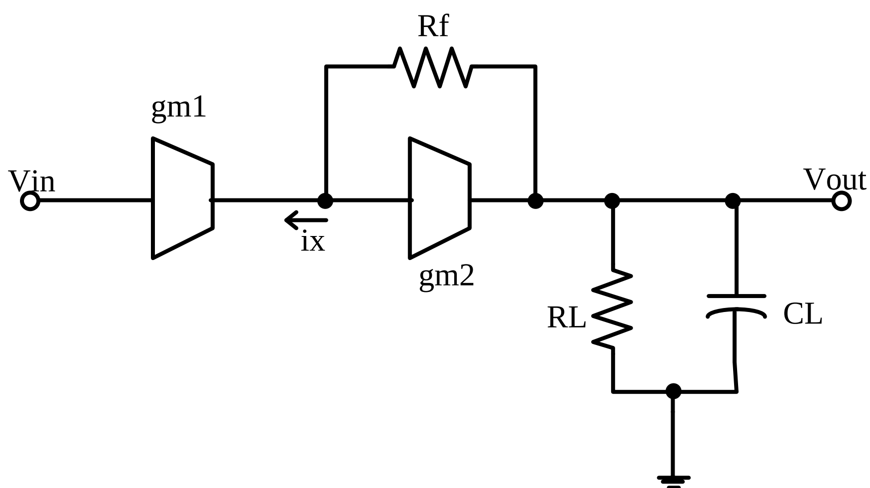

Fig. 9: The basic Cherry-Hooper topology.

$$i_x = v_{in} g_{m1} \tag{2.71}$$

$$v_0/v_{in} = \left(g_{m2}R_f - 1\right)\left(\frac{g_{m1}R_l}{1 + g_{m2}R_l}\right)\frac{1}{1 + \frac{sR_lC_l}{1 + g_{m2}R_l}} \tag{2.72}$$

$$Assume\ g_{m2}R_l \gg 1$$

$$H(s) \cong \frac{g_{m1} R_f}{1 + \frac{sC_l}{g_{m2}}} \tag{2.73}$$

$$gain = g_{m1} R_f \tag{2.74}$$

$$\omega_{-3dB} = {}^{g_{m2}}\!/_{C_l} \tag{2.75}$$

As shown in equations 2.74 and 2.75 the gain and bandwidth of the amplifier are unrelated. The gain only depends on the feedback resistor (R_f) and g_{m1} while the bandwidth only depends on g_{m2} and the load capacitance (C_l). This means that gain is no longer sacrificed to increase bandwidth and visa-versa. A schematic of the CH amplifier is shown in figure 10 to help highlight the drawback of the design.

Comparing the schematic to figure 9 g_{m1} is the transconductance of M1 and g_{m2} is the transconductance of M2 while the rest of the components have the same name. To increase the gain either R_f or g_{m1} must be increased. If R_f is increased too much the voltage at the gate of M2 will be low which reduces the output dynamic range. Increasing g_{m1} requires I_1 to increase which increases the current through R_l and R_f which reduces the output common mode voltage and dynamic output range. The current through R_l can be reduced by a reduction in g_{m2}, but this will decrease the bandwidth and returns to the design to the same gain or bandwidth tradeoff.

The bandwidth suffers the constraint as the gain. The load capacitance cannot be controlled by the designer which only leaves g_{m2} to control the bandwidth. An increase in g_{m2} requires raising the current I_2 resulting in a larger voltage drop across R_l lowing the output common mode. The resistor R_l can be reduced to compensate for the increased current, but it must remain larger than $1/g_{m2}$. The only to increase both gain and bandwidth is to increase the power supply voltage which is not an option for a specified CMOS technology.

The Cherry-Hooper design essentially moves the design tradeoff from gain and bandwidth to gain/bandwidth and dynamic range. The modified Cherry-Hooper is presented next which alleviates this tradeoff.

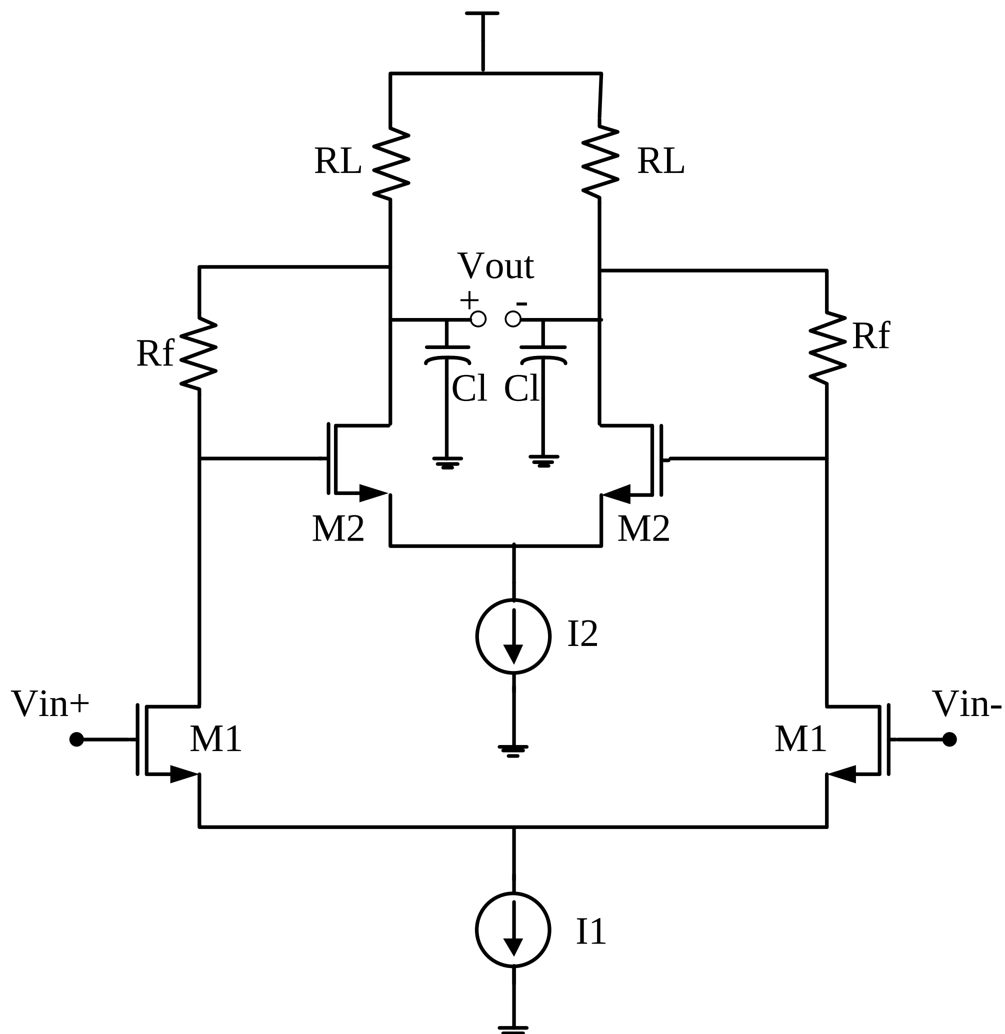

Fig. 10: Schematic of a Cherry-Hooper amplifier.

2.8 Modified CHERRY-HOOPER DESIGN

The limitation placed on the amplifier by the dynamic range can be reduced by using a modified CH topology as shown in figure 10. A resistor divider made by R_1 and R_2 is added to the feedback path. This means that only a fraction of the output voltage is buffered fed back to the input. This allows the designer to increase the gain of the amplifier as shown below without increasing R_f or g_{m1} so there is no output dynamic range sacrifice.

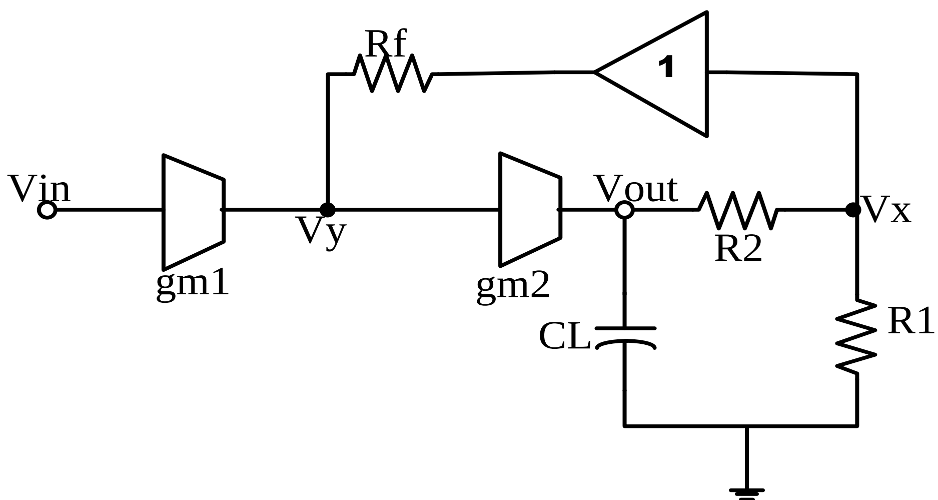

Fig. 11: Modified Cherry-Hooper topology.

$$v_x = v_{out}\frac{R_1}{R_1 + R_2} \tag{2.76}$$

$$v_y = \frac{-v_{out}}{g_{m2}\left(\frac{R_1 + R_2}{1 + sC_L R_L}\right)} \tag{2.77}$$

$$H(s) = g_{m1}R_f\left(\frac{g_{m2}R_L}{1 + g_{m2}R_1}\right)\frac{1}{1 + \frac{sR_L C_L}{1 + g_{m2}R_1}} \tag{2.78}$$

$$Assume\ g_{m2}R_1 \gg 1$$

$$H(s) \cong g_{m1}R_f\left(1+\frac{R_2}{R_1}\right)\left(\frac{1}{1+\frac{sC_L}{g_{m2}}\left(1+\frac{R_2}{R_1}\right)}\right) \tag{2.79}$$

$$gain = g_{m1}R_f\left(1+\frac{R_2}{R_1}\right) \tag{2.710}$$

$$f_{-3dB} = \frac{g_{m2}}{C_L\left(1+\frac{R_2}{R_1}\right)} \tag{2.711}$$

Equations 2.710 and 2.711 show the gain and -3dB point of the modified CH amplifier. The gain is now increased by a factor of R_2/R_1 while the bandwidth is reduced by the same factor. Figure 12 shows a schematic for a modified CH amplifier in CMOS. The added resistor divider is done with R2 and R3 while M3 acts as a unity gain amplifier to isolate the feedback from the output. This allows for the current through R1 and R2 to only come from I2 which helps improve the dynamic range.

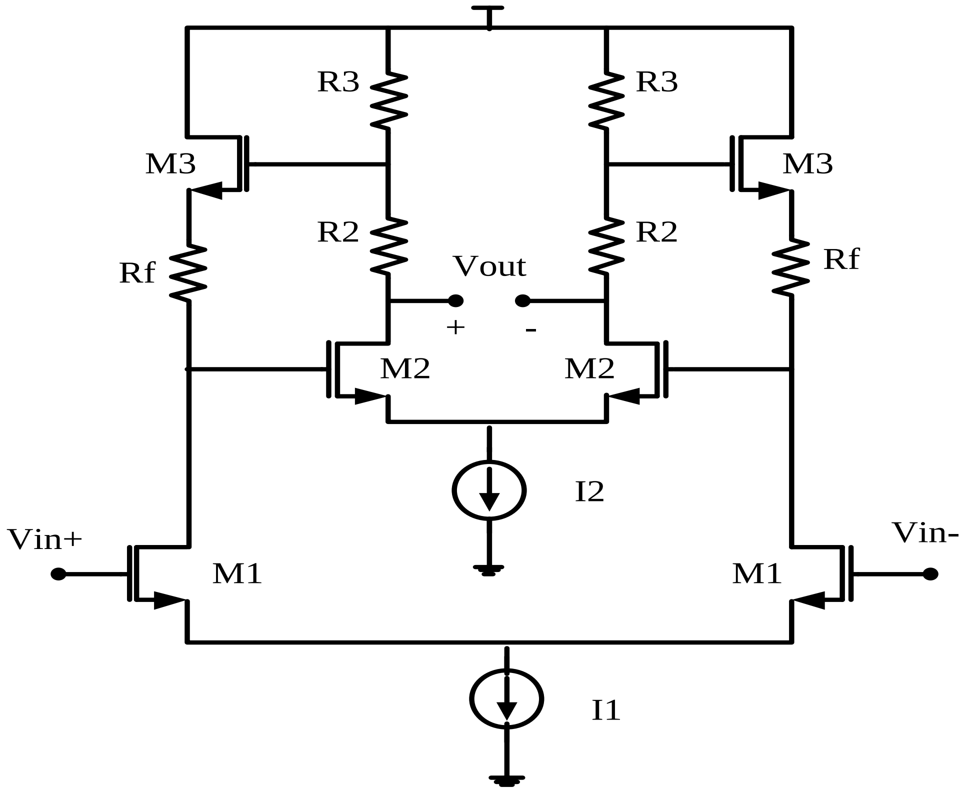

Fig. 12: A schematic of a modified CH amplifier.

With this schematic the gain can be improved by increasing I1 and g_{m1}. To keep the dynamic range constant R_f must be reduced. This loss in gain from reducing R_f can be compensated for by increasing the ratio of R_2 to R_1. To make up for the bandwidth decrease caused by R_2 and $R_{1,}$ I_2 can be increased. The absolute value of R_1 and R_2 can be decreased to keep the output voltage constant since only the ratio of the two impacts the gain and bandwidth. The only drawback is that g_{m2}*R_1 must be much greater than one. This puts a limit on how large I_2 can be.

2.9 MODIFIED CHERRY-HOOPER AS A TIA

The modified CH amplifier can be easily adapted to a TIA design by replacing g_{m1} with a common gate or regulated gate cascade input stage. This topology with a common gate input is shown in figure 13. The input stage acts as a buffer stage to provide low input impedance. As discussed in section 2.5 this helps avoid the parasitic capacitance from the photodiode determining the bandwidth of the system.

$$v_x = v_{out}\frac{R_1}{R_1 + R_2} \tag{2.81}$$

$$v_y = \frac{-v_{out}}{g_m(R_1 + R_2)} \tag{2.82}$$

$$v_y - v_x = R_f i_{in} \tag{2.83}$$

$$Z_T = \frac{v_o}{i_{in}} = R_f\left(\frac{R_1 + R_2}{R_1 + {}^1/_{g_m}}\right) \qquad \text{(2.84}$$

$$Assume\ {}^1/_{g_m} \ll R_1$$

$$Z_T \cong -R_f\left(1 + \frac{R_2}{R_1}\right) \tag{2.85}$$

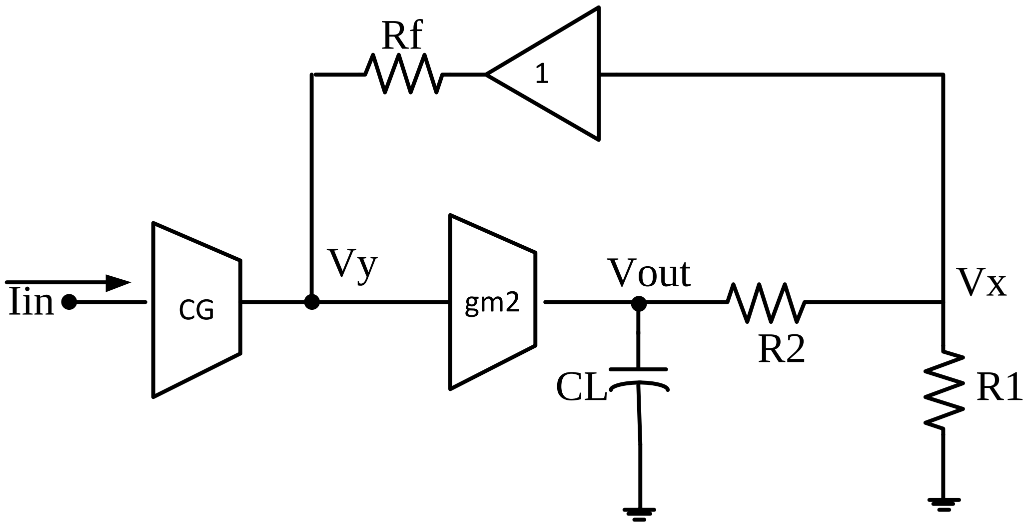

Fig. 13: A modified CH TIA with a common gate input stage.

The modified CH TIA must be treated as a two pole system. The two high impedance nodes are at V_y and V_{out}. The pole created at the output is defined in equation 2.86 while the pole at V_y is defined in equation 2.87. The quality factor, Q, and the center frequency of the amplifier at listed in equations 2.88 and 2.89. A higher value of Q will provide a wider bandwidth with more peaking and ringing at the output. A low Q value will create an over damped system. Having Q=0.707 will provide the maximally flat response while $Q = {}^{1}\!/_{\sqrt{3}}$ as described in [5] will provide the ideal compromise between peaking and bandwidth.

$$\omega_{p1} = \frac{-1}{(R_1 + R_2)C_L} \tag{2.86}$$

$$\omega_{p2} = \frac{-[1 + g_m(R_1 + R_2)]}{R_f C_y} \tag{2.87}$$

$$Q = \frac{\sqrt{R_f C_y C_L (R_1 + R_2)(1 + g_m R_1)}}{R_f C_y + [C_L (R_1 + R_2)(1 + g_m R_1)]} \tag{2.88}$$

$$Center\ Frequency\ \omega = \sqrt{\frac{1 + g_m R_1}{R_f(R_1 + R_2)C_y C_L}} \quad (2.89)$$

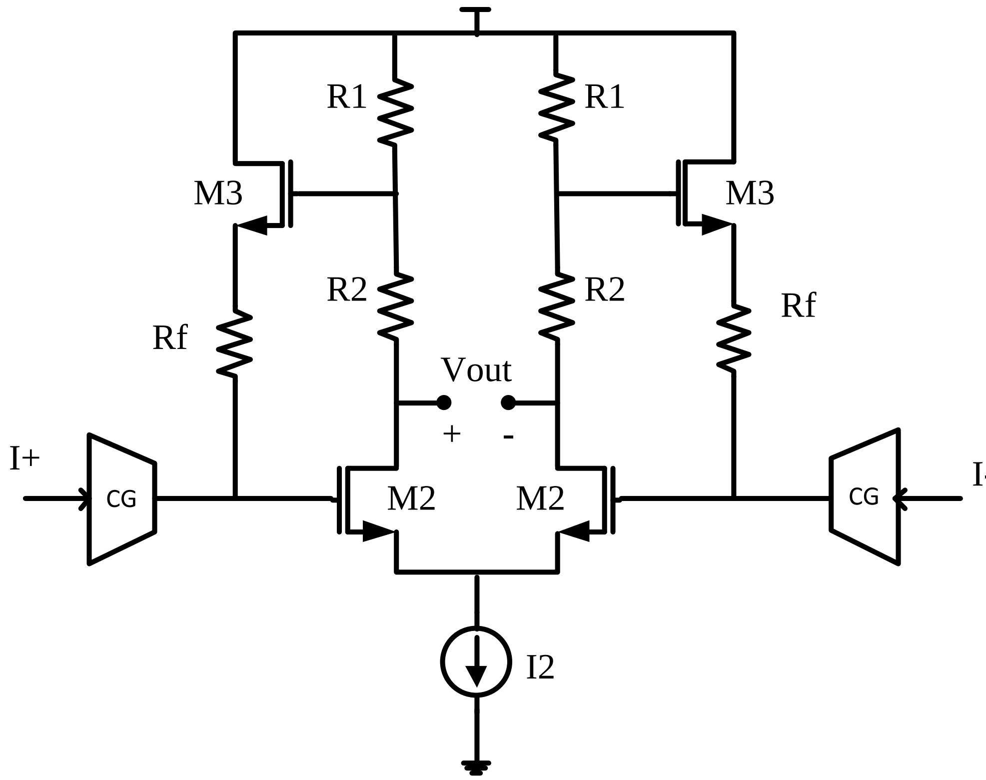

Fig. 14: Schematic of a modified CH TIA.

The easiest way to analyze the noise is to see by inspection that the modified CH TIA is very similar to the common gate topology. It uses a common gate input followed by a voltage amplifier.

The second stage is similar to a shunt-shunt architecture which has a much lower input referred noise than the common gate. For this design the noise is dominated by the active devices in the common gate block and the feedback resistance. Since the feedback resistance is a major contributor to the input referred noise, the smaller value used in the modified CH creates a higher amount of noise. The total input referred noise spectral density from the major contributors is listed below.

$$\overline{i_{in,n}^2} = \gamma k_B T g_{m,cg} + \frac{4k_B T}{R_f} \quad (2.811)$$

2.10 LITERATURE REVIEW

There are many factors that make it difficult to compare TIA designs. Many are designed as an analog front end for digital communications while few are designed for use with an analog to digital converter for signal processing. This leads to many different designs optimized in a variety of ways. Digital communication receivers focus on high gain and wide bandwidth with noise and linearity considerations only required to keep the BER low. A sampled analog design has much stricter noise and linearity specifications and therefore have lower gain bandwidth product. Naming conventions for the different topologies also present another issue. It is common for one paper to refer to an amplifier as a regulated gate cascade while it is actually a Cherry Hooper design with an RGC input followed by a voltage amp with shunt-shunt feedback. Any design in this comparison labeled combination is some form of common gate input followed by a voltage amplifier with shunt feedback.

Table 2: Comparison of state of the art TIAs.

Reference	**Topology**	**Technology**	**Gain**	**Bandwidth**	**Noise**	**C_{PD}**
[4]	RGC	.6µ	58dBΩ	860MHz	6.3pA/$\sqrt{Hz}$	
[6]	Combination	.18µ	87dBΩ	7.6GHz	NR	

[7]	Combination	.18µ	52dBΩ	3.9GHz	NR	
[8]	Combination	.25µ	80dBΩ	670MHz	13pA/$\sqrt{Hz}$	
[9]	Combination	.35µ	66dBΩ	256MHz	NR	
[10]	RGC	.8µ	120dBΩ	58MHz	.5pA/$\sqrt{Hz}$	
[11]	Combination	.13µ	52dBΩ	4.2GHz	NR	
[12]	Shunt-Shunt	.18µ	70dBΩ	1GHz	4.5pA/$\sqrt{Hz}$	

CHAPTER 3 IMPLEMENTATION OF A BANDPASS TIA

3.1 SERVO LOOP DESIGN

Photodiodes rarely operate in complete darkness with only the signal present. With this in mind any analog implementation requires some way to reject the low frequency signal from the ambient light. DC blocking caps are the most common way to block this unwanted current, but there are issues with this as described in [11]. This design utilizes a servo loop instead of a DC blocking cap. A servo loop essentially is an integrator in the feedback path. This provides a large amount of negative feedback at low frequencies and no feedback at high frequencies. The concept for a voltage amplifier is shown in figure 15.

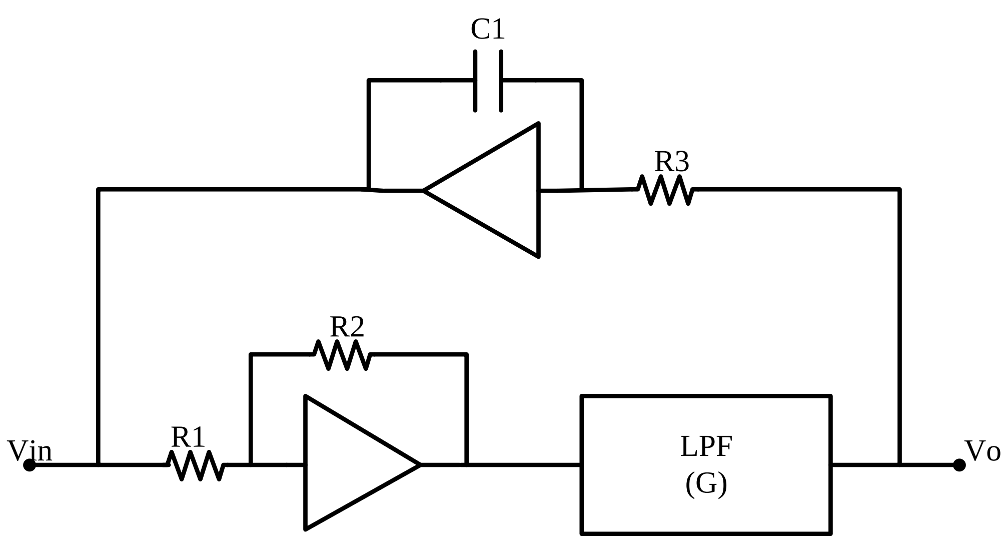

Fig. 15: A block diagram of a voltage amplifier with a servo loop.

An analysis of the above circuit is easiest if the gain of the low pass filter (G) is assumed to be -1 and has a -3dB point more than a decade beyond high pass -3dB. The transfer function is shown in equation 3.10.

$$\frac{v_{out}}{v_{in}} = -G_{LPF} * \frac{R_1 + R_2}{R_2} * \frac{s\frac{R_2 R_3 C_L}{R_1}}{1 + s\frac{R_2 R_3 C_L}{R_1 G_{LPF}}} \tag{3.10}$$

From the transfer function it can be seen that the in band gain is the same as it would be without the servo loop. The high pass 3dB frequency is shown in equation 3.11.

$$f_{3dB} = \frac{{}^{R_1}/_{R_2}\, G_{LPF}}{2\pi R_3 C_L} \tag{3.11}$$

The high pass 3dB point is the pole of the feedback integrator multiplied by the loop gain of the circuit. This means that the larger the forward path gain the larger the RC of the integrator will need to be for the same high pass response.

3.2 CIRCUIT OVERVIEW

A block diagram of the circuit is shown in figure 16. It is composed of a modified CH TIA with an RGC input followed by a low pass filter. The servo loop feedback is made of an integrator followed by an OTA which converts the integrator's output voltage to a current. The transimpedance gain is primarily achieved in the TIA, the low pass filter was added to increase the dynamic range of the output and create a controlled low pass -3dB frequency. The transfer function of the circuit is the same as the servo loop presented in section 3.1 with the high pass 3dB frequency equal to the RC time constant of the integrator multiplied by the loop gain of the circuit. The interesting thing in the proposed circuit is the gm of the OTA in the feedback can be used to reduce the loop gain of the circuit which helps reduce the size of R3 and C2.

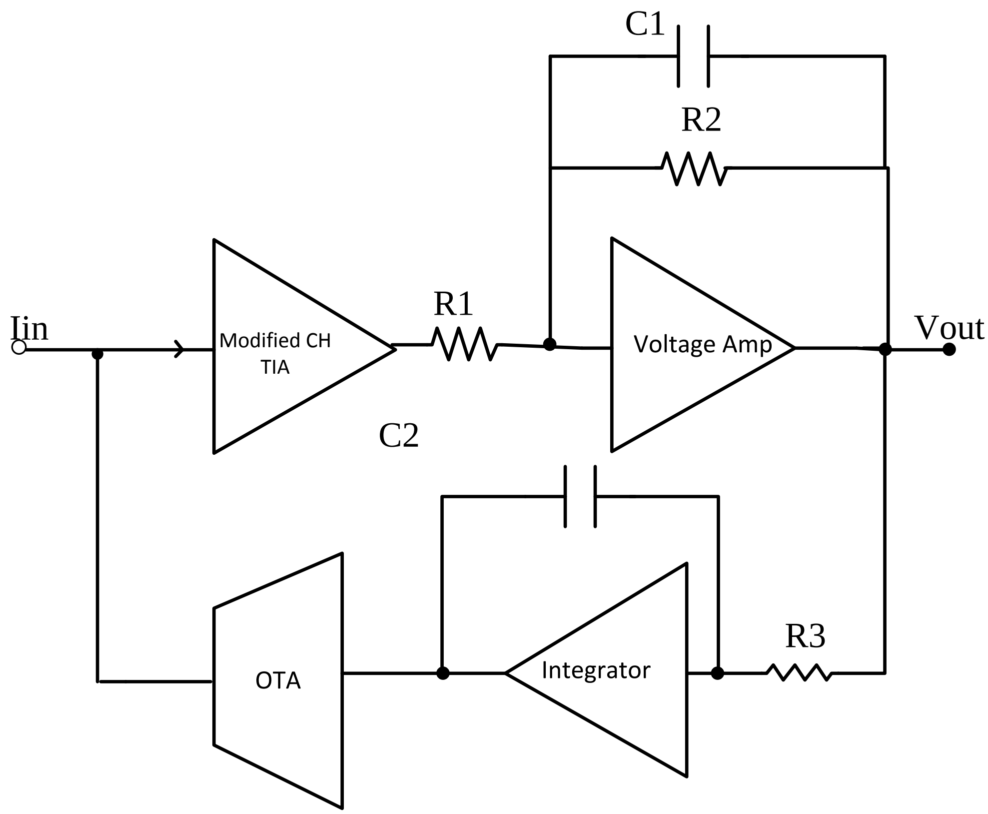

Fig. 16: Block diagram of the presented design.

Table 3: List of equations that define the presented circuits parameters.

Parameter	**Equation**
Forward Gain	$Gain = Z_T * \left(\frac{R_2}{R_1}\right)$
Loop Gain	$Gain_{CL} = Z_T * \left(\frac{R_2}{R_1}\right) * g_m$
Low Pass -3dB Frequency	$f_{-3dB} = \frac{1}{2\pi R_2 C_1}$

High Pass 3dB Frequency	$$f_{3dB} = \frac{Z_T\left(\frac{R_2}{R_1}\right)g_m}{2\pi R_3 C_2}$$

3.3 DESIGN SPECIFICATIONS

The requirements of the circuit are presented in the table below.

Table 4: Design specifications for the TIA.

Parameter	**Specification**
Transimpedance Gain (Z_T)	210kΩ
Input Impedance (C_{PD})	0.8pF
Input Dynamic Range	4nA to 4µA
Output Dynamic Range	1mV to 1V
Input Referred Noise Density	0.35$pA/\sqrt{Hz}$
Bandwidth	15MHz to 35MHz
Gain Bandwidth Product	6.3THz*Ω
Dark Current	0 to 40µA

3.4 MODIFIED CHERRY-HOOPER TIA

Small devices were used throughout the design to allow for as wide a bandwidth as possible. The dominant pole in the design occurs at V_x with the second pole at the output. The bias currents through the RGC input were also small to try and minimize noise. The current I_1 is 18µA while the current I_2 is 80µA. The Q value calculated using equation 2.88 is Q≈0.5 and the center frequency is ω=1.3x10^9 rad/s or f=192MHz. The calculated gain using equation 2.85 is Z_T=167kΩ. The actual gain of the circuit is lower because the assumption that ${}^{1}/{}_{g_{m7}} \ll R_1$ is not true. Even if the simplified gain equation were valid the gain is still lower than the design requirement. The rest of the gain is made up for in the voltage amplifier.

This stage plays a large part in setting the input referred noise of the entire circuit. Equation 2.811 defines the noise of this amplifier and highlights the primary drawback of the design. To avoid having the photodiode capacitance define the bandwidth of the system the input impedance must be low and low input impedance increases the noise. Pushing the pole at V_x to higher frequencies requires a smaller feedback resistance. The gain is held constant by increasing the ratio of R_2 to R_1, but the noise is increased. All of the benefits the modified CH provides to increase the gain and bandwidth come with the penalty of increased noise. A rough estimate of the input referred noise is shown below. This low estimate already puts the noise ten times higher than the requirement.

$$\overline{\iota_{n,\iota n}^2} = \gamma k_B T g_m + \frac{4k_B T}{R_f} \cong 12 * \frac{10^{-24}A^2}{Hz} \tag{3.40}$$

$$OR$$

$$\overline{\iota_{n,\iota n}} = 3.5pA/\sqrt{Hz}$$

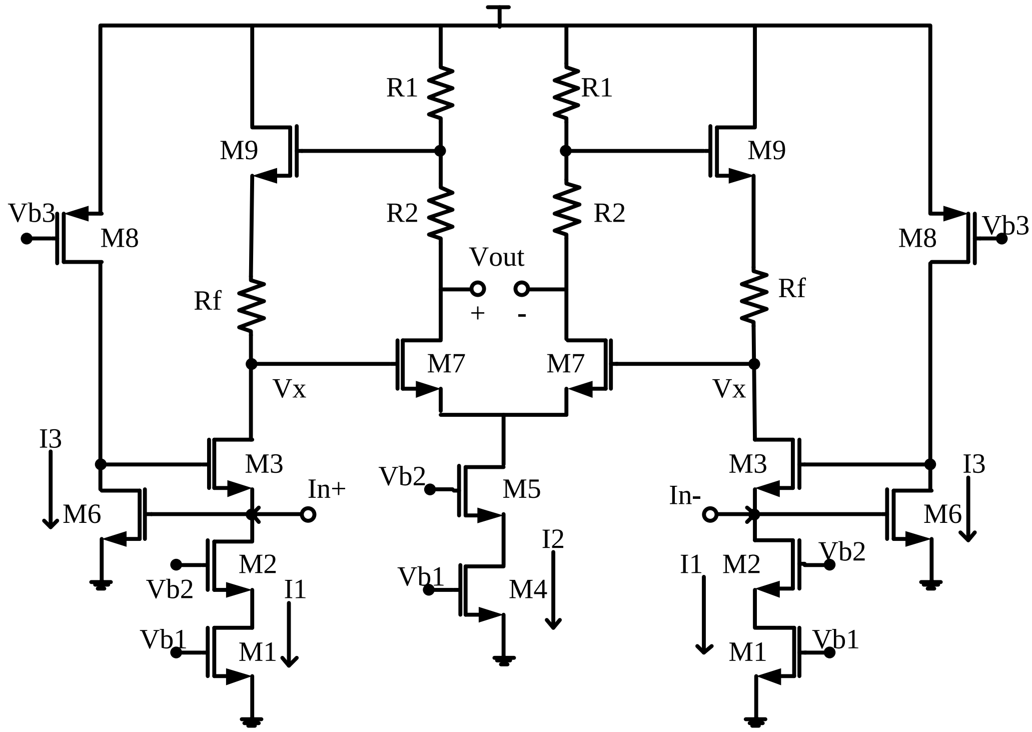

Fig. 17: Schematic of the presented TIA.

Table 5: Transistor sizes used in the TIA.

Transistor	**Width (W)**	**Length (L)**
M1	1.62µ	0.36µ
M2	0.9µ	0.18µ
M3	5.04µ	0.18µ
M4	7.56µ	0.36µ
M5	5.04µ	0.18µ
M6	2.52µ	0.18µ
M7	5.04µ	0.18µ
M8	5.04µ	0.18µ
M9	5.04µ	0.18µ

Table 6: Resistor values for the TIA schematic.

Resistor	Value
R_f	20kΩ
R_1	1.8kΩ
R_2	15kΩ

3.5 OP AMP DESIGN

The opamp used in this design is a standard and well known design. It is fully differential with a cross coupled class AB output stage. The design is shown in figure 18, but since it is not critical portion further analysis is not shown. The interested reader can find further details of the design in [3].

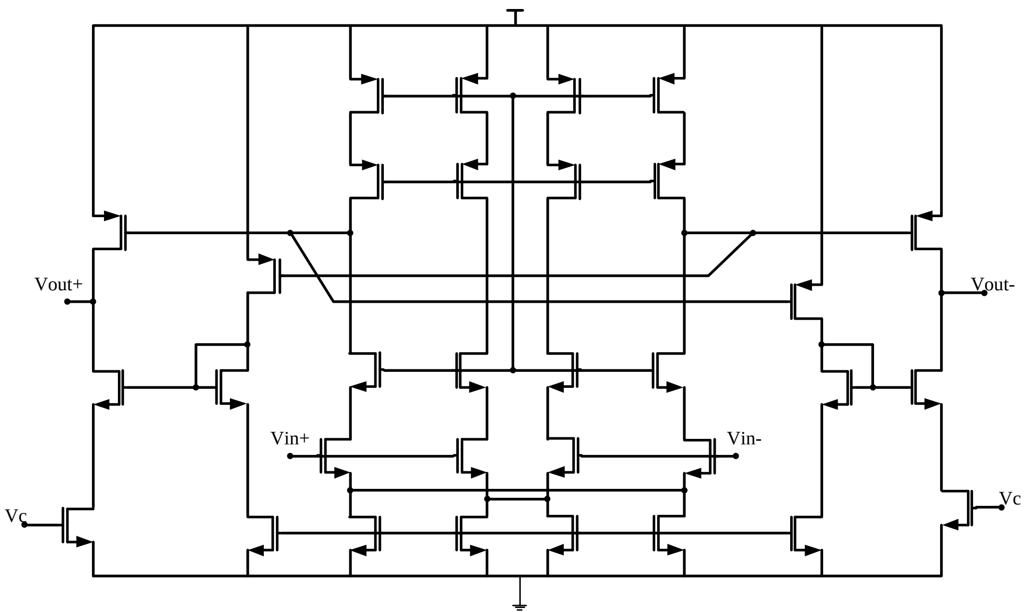

Fig. 18: Schematic of the opamp used in the LPF.

3.6 INTEGRATOR DESIGN

As with the opamp the integrator is not a new design. The same opamp could have been used here, but there was a plan to attenuate the output voltage before connecting it to the feedback to lower the size of the RC network. This attenuation would have shifted the DC level of the input to the integrator nearly to ground. With this in mind a PMOS input pair was used to accommodate the low input voltage. It is a standard folded cascade amplifier.

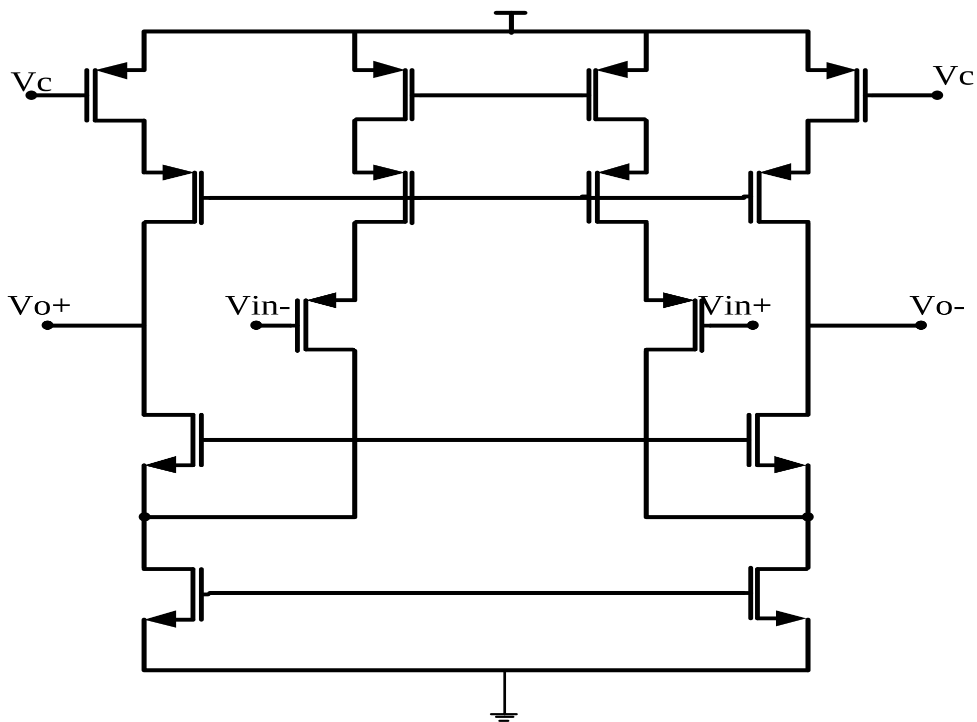

Fig. 19: Schematic of the amplifier used in the integrator.

3.7 OTA DESIGN

The OTA is an important part of the design. It sets the transconductance of the feedback which takes part in determining where the high pass 3dB frequency is. Since the output of the OTA is directly connected to the input of the TIA any output current noise directly contributes to the input referred noise. This creates a dilemma because the bias current through the output branch sets the limit to how large of a DC current offset can be cancelled and the larger the bias current the larger the output noise. A source degenerated telescopic cascode was used to keep the trans conductance low with a large enough bias current to sink any DC current at the input of the TIA. No common mode feedback was necessary for the design since it is DC coupled to the RGC input of the TIA which sets the voltage level.

Source degeneration helps control the transconductance of the amplifier while also linearizing its response. With the resistor in place G_m is equal to the following equations.

$$G_m = \frac{g_{m1}}{1 + g_{m1} R_S} \tag{3.71}$$

$$If\ g_{m1} R_s \gg 1, then$$

$$G_m = \frac{1}{R_S} \tag{3.72}$$

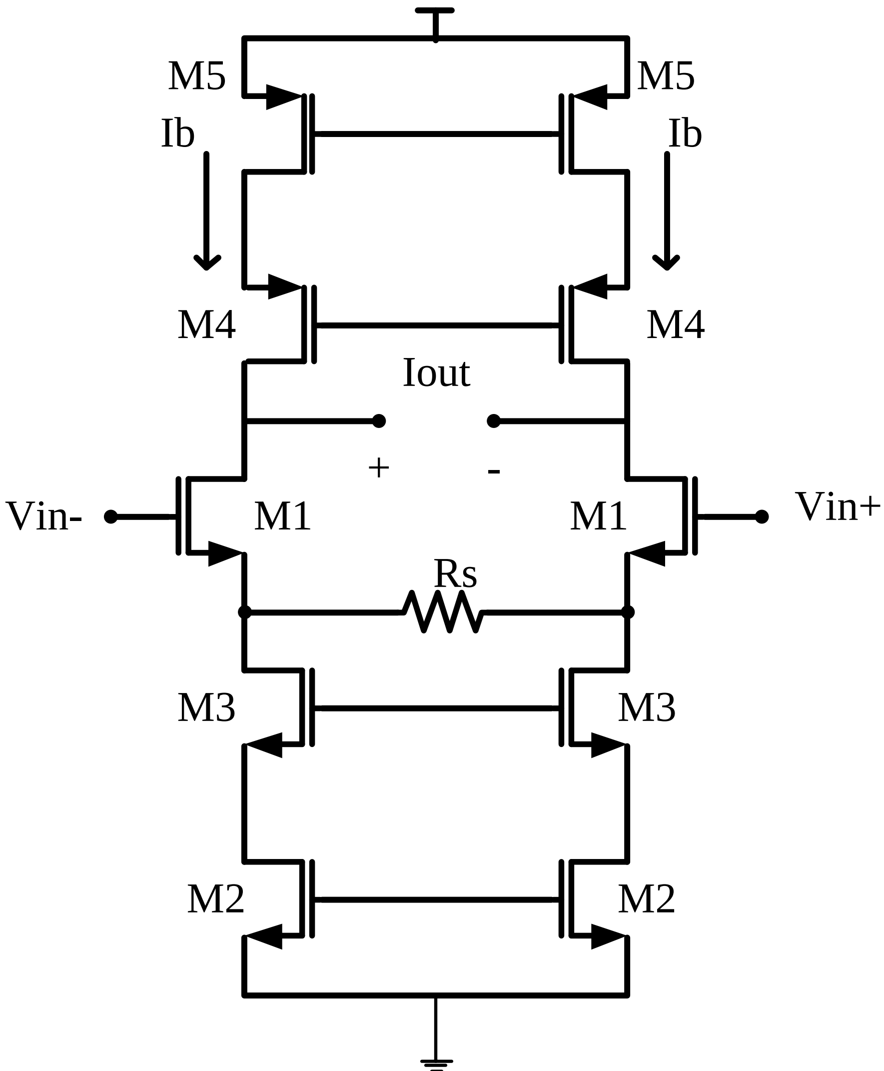

Fig. 20: Schematic of the transconductance amplifier used.

The output must be able to cancel out all of the dark current from the photodiode. For this design the current can be as large at 40μA. To ensure the OTA is able to sink that much current the bias I_b must be much larger than dark current. A larger bias current results in more noise at the output and the source degeneration does not reduce thermal since it only reduces the differential transconductance of the circuit. With this design the current noise of each device directly adds to the output of the amplifier. The total output thermal noise is calculated in equation 3.71.

$$\overline{i_{n,out}^2} = \gamma k_B T g_{m1} + \gamma k_B T g_{m2} + \gamma k_B T g_{m3} + \gamma k_b T g_{m4} + \gamma k_b T g_{m5} \tag{3.71}$$

$$\overline{i_{n,out}} \cong 5.5 pA/\sqrt{Hz}$$

CHAPTER 4 SIMULATION RESULTS

4.1 TIA CHARACTERIZATION

With the servo loop design the photodiode is DC coupled to the input of the TIA. Because of this the bias voltage across the diode is fixed by the input common mode voltage of the TIA. The downside is the diode cannot be placed across the differential inputs of the TIA and have a reverse DC bias. Figure 21 shows the test bench used in simulation. There is no available model for the photodiode available so another diode made with the same process was used to mimic any leakage current. The capacitor C1 is the parasitic capacitance of the photodiode while C2 is connected to the other input to balance the two.

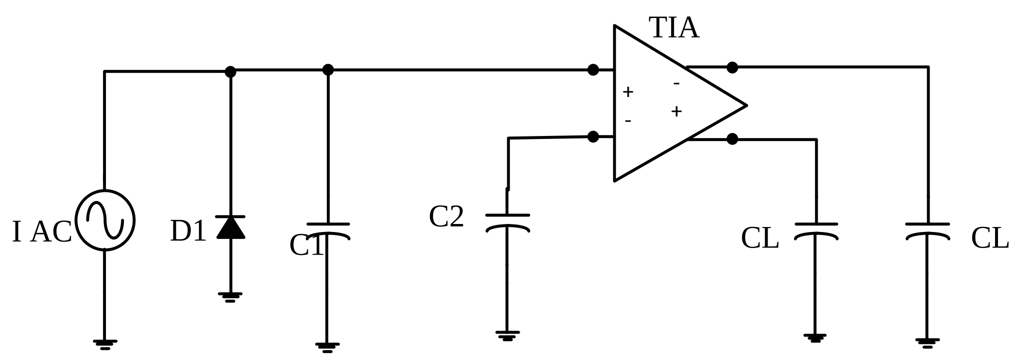

Fig. 21: Test bench for the TIA.

The –3dB frequency and gain for the TIA are shown in figure 22. The gain is 70.8kΩ (97dBΩ) and the roll off frequency is 98MHz. The system gain specification is 210kΩ and the TIA alone does not achieve this. The LPF provides the rest of the gain for the system. The input referred noise spectral density is shown in figure 23. In the pass band the noise varies from 3 $pA/\sqrt{Hz}$ to

$3.75\ pA/\sqrt{Hz}$ which closely agrees with the thermal noise calculated in equation 3.40.

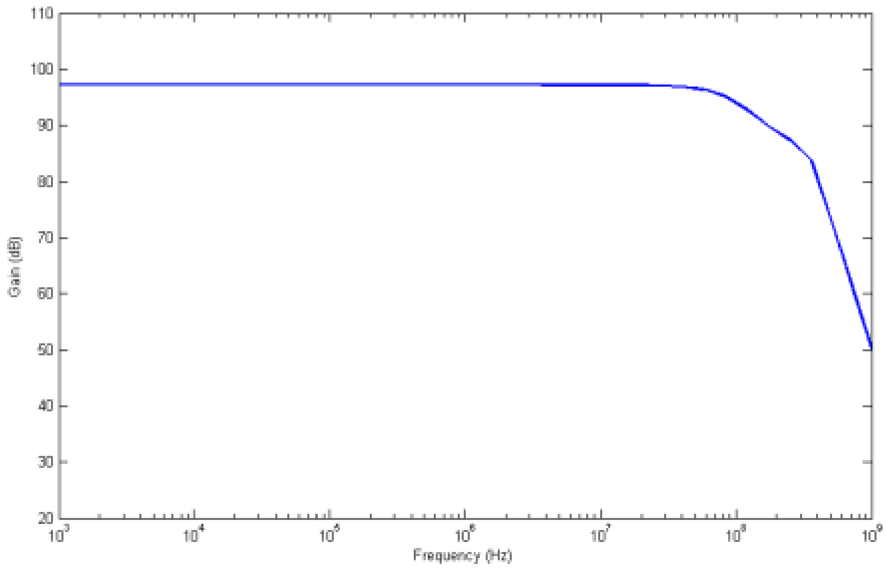

Fig. 22: Gain and bandwidth of the TIA.

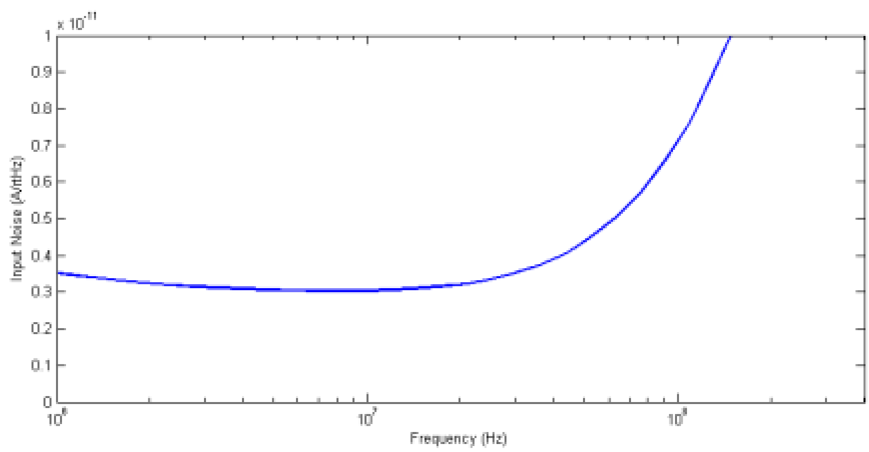

Fig. 23: Input referred noise of the TIA.

The distortion of the TIA should also set the total distortion of the circuit. It is performing a single ended to differential conversion which causes the distortion to be largely based on the bias current of the input device. This bias current was intentionally made low to lower the noise of the amplifier, but also must be high to avoid distortion issues. The plot below shows the intermodulated distortion caused by two input signals with half the input dynamic range. The frequency of these signals are 20MHz and 21MHz. While there was no given specification for linearity the goal was to get the IMD below 70dB.

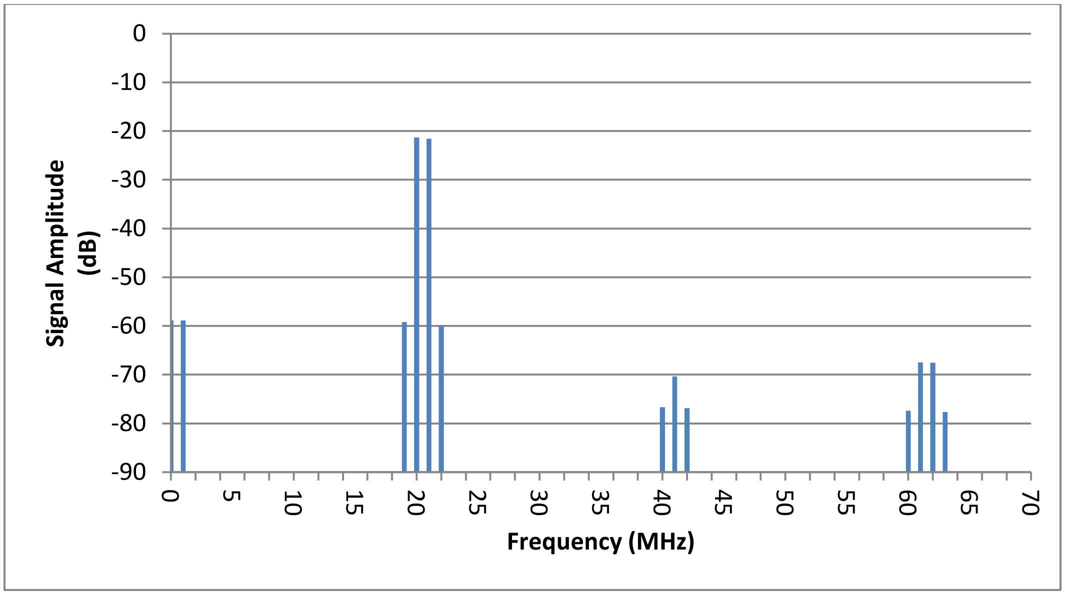

Fig. 24: Third order intermodulated distortion of the TIA.

4.2 CHARACTERIZATION OF THE LPF

The main purpose of the LPF is to set the low pass -3dB frequency and provide a large output signal swing. It also must not limit the circuit in any way. For this to be true the distortion of the filter must be less than the TIA distortion and the noise must be a minor contributor to the overall input referred noise. Figure 25 shows the test bench for the LPF. For the distortion simulation the input voltage was set to the maximum output swing of the TIA. In this test that swing is

$4\mu A * Z_T$ which is $285mV_{p\text{-}p}$. The gain of the LPF is set to 4 to provide a $1.14V_{p\text{-}p}$ output voltage which is slightly more than the $1V_{p\text{-}p}$ specification.

To measure the LPF's impact on the overall noise it must be referred back to the input of the TIA. This is done by dividing the input referred noise of the LPF by the transimpedance gain of the TIA as shown in equation 4.21.

$$\overline{i_{n,TIA}} = \frac{\overline{v_{n,LPF}}}{Z_T} \tag{4.21}$$

The noise spectral density at the TIA input caused by the LPF is shown in figure 27. The noise is much smaller than the total input referred noise of the system so the LPF is minor contributor.

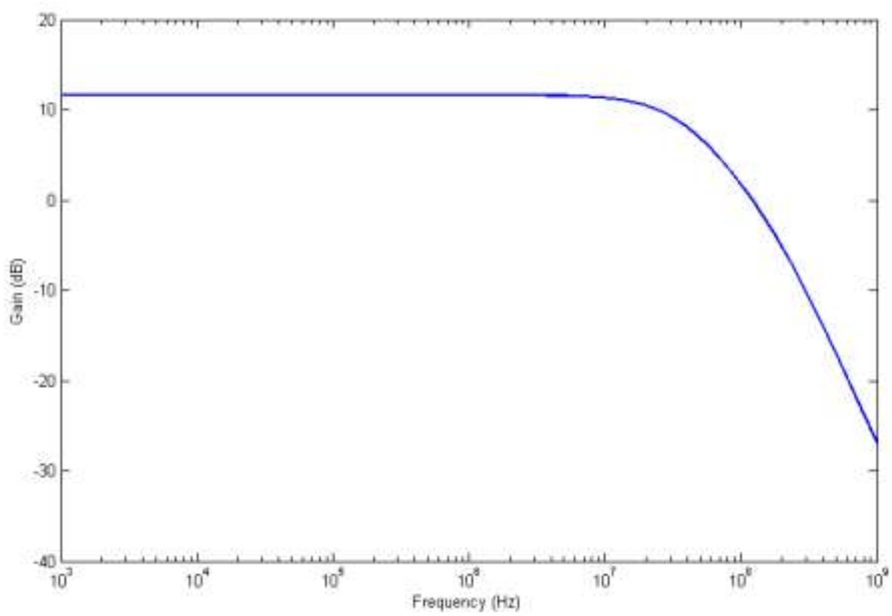

Fig. 25: Gain and bandwidth of the LPF.

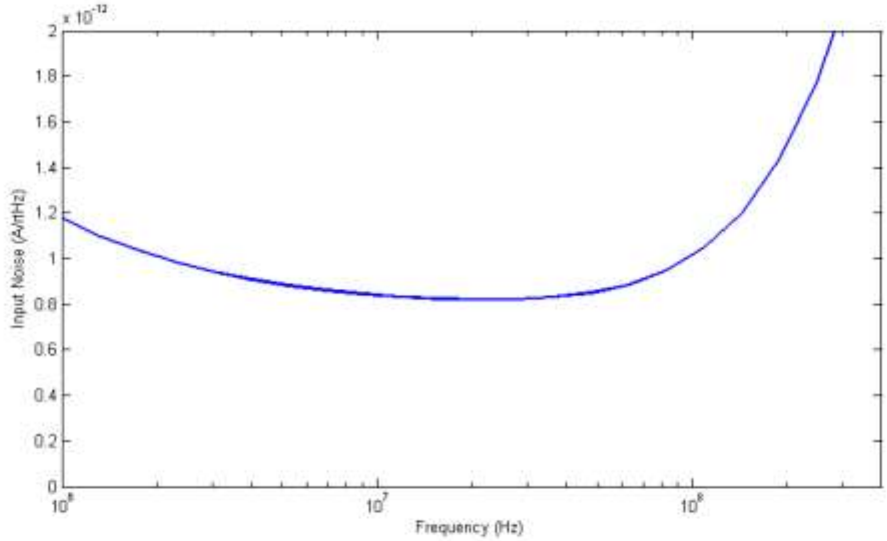

Fig. 26: Input referred noise at the TIA caused by the LPF.

4.3 CHARACTERIZATION OF THE INTEGRATOR

The integrator sets the 3dB high pass frequency and is subject to the same constraints as the LPF. The noise must not be a major contributor and the distortion must also be less than the TIA distortion. Because it is in the feedback loop the output referred noise of the circuit is important. The output referred voltage noise of the integrator is multiplied by the G_m of the OTA to calculate the input referred noise of the TIA.

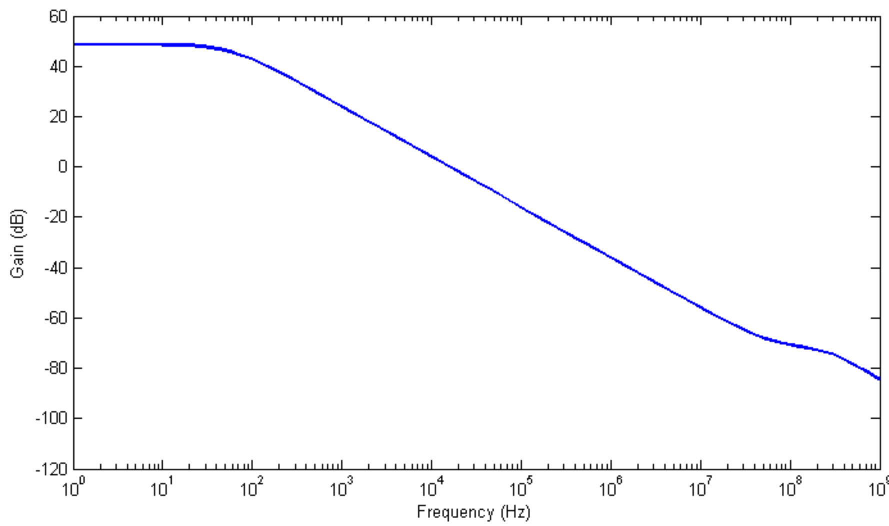

Fig. 27: Gain and bandwidth of the integrator.

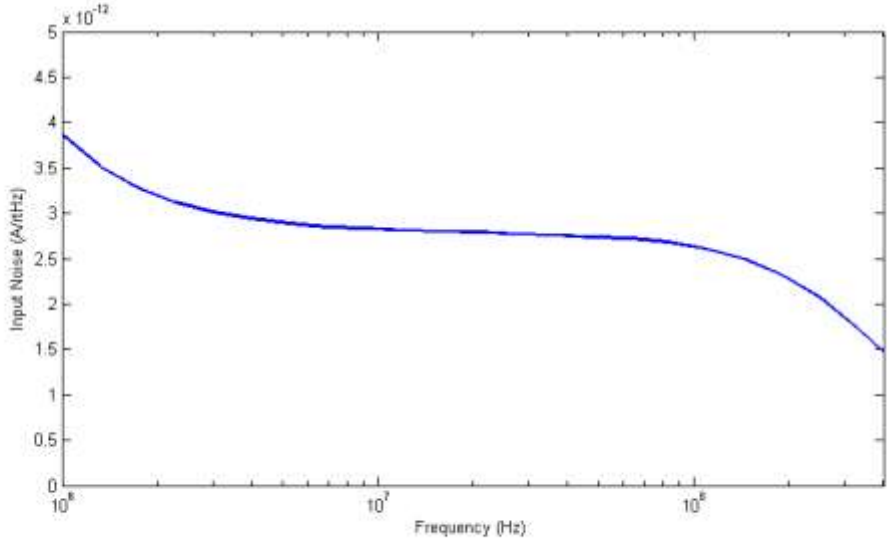

Fig. 28: The spectral density of the integrator noise referred to the TIA input.

4.4 CHARACTERIZATION OF THE OTA

The purpose of the OTA is to convert the feedback voltage to a current. The important parameters for this stage are the transconductance and input referred noise. Since the output is directly connected to the input of the TIA any noise in this circuit will be a major contributor to the total input referred noise. The output noise current density was calculated by simulated the input referred noise of the circuit and multiplying it by the transconductance of the circuit. At low frequency the flicker noise of the active devices is dominant. Once the thermal noise dominants it closely matches the noise calculated in equation 3.71 of 5.5 $pA/\sqrt{Hz}$.

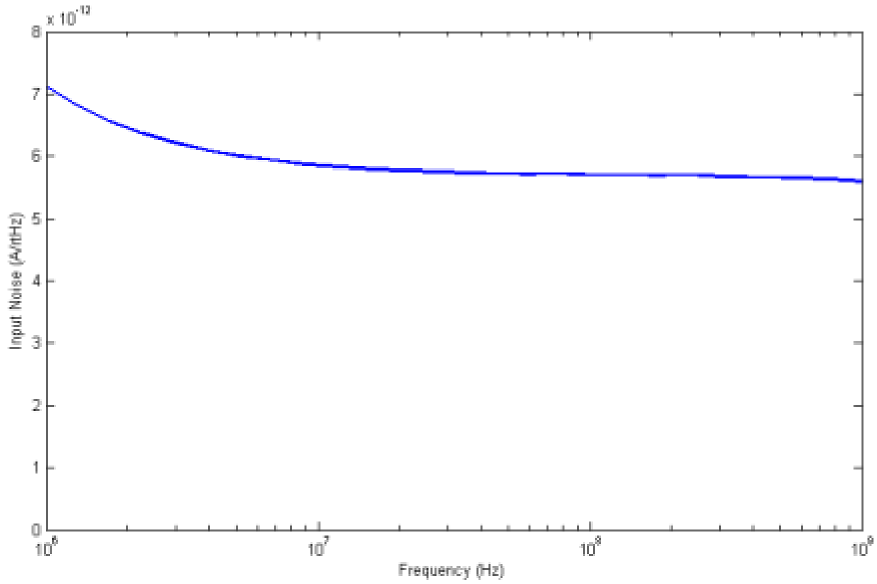

Fig. 29: The spectral density of the OTA noise referred to the input of the TIA.

4.5 CHARACTERIZATION OF THE COMPLETE CIRCUIT

The gain and bandwidth of the complete system are shown in figure 31. From it the high pass 3dB frequency is 5MHz, while the low pass -3dB frequency is 45MHz. The frequencies are wider than the required bandwidth of the system to avoid any compression within the passband. If a more tightly controlled bandwidth is required higher order analog filters may be used or digital filtering techniques can be employed after the ADC. The peak gain in the passband is about 106dBΩ or 200kΩ. This is slightly below the required gain and can be attributed the loading of the TIA by the LPF.

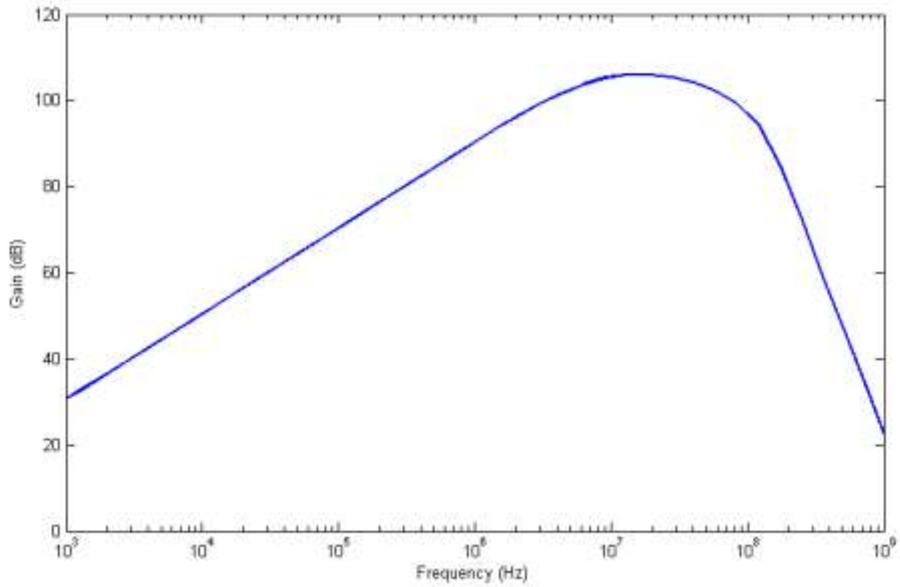

Fig. 30: Gain and bandwidth of complete circuit.

One method for testing the DC offset cancellation is to provide a stair step input current and monitor the output. The benefit to this method is that it also tests the design for stability. If the phase margin of the design was too low ringing would be present at the output. A small amount is noticed when the input current jumps from 32µA to 40µA. This is mostly likely caused by the output of the OTA saturating. The high pass and low pass frequencies can be extracted by measuring the rise and fall times of the output.

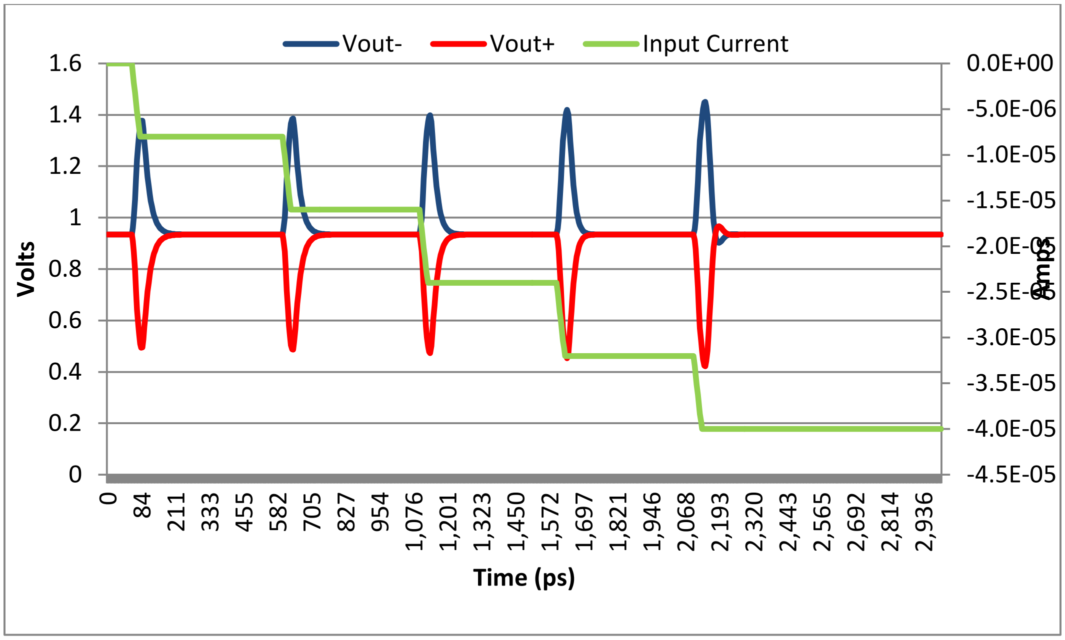

Fig. 31: Transient simulation of complete current showing DC offset cancellation and stability.

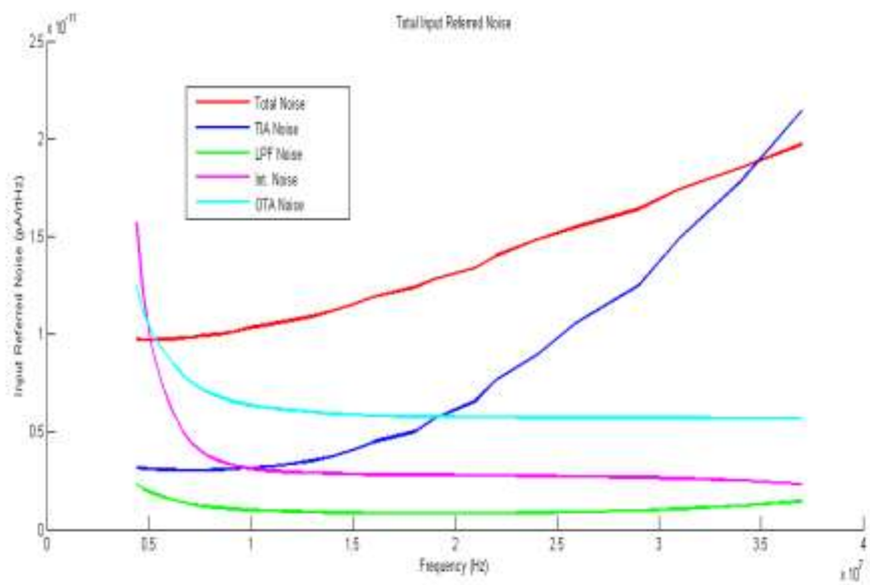

Fig. 32: Superposition of all noise sources compared to total input referred noise.

Figure 33 shows how much each circuit block contributes to the total input referred noise of the system in the pass band. It shows the OTA is the primary source of noise until higher frequencies where the TIA becomes the dominant contributor.

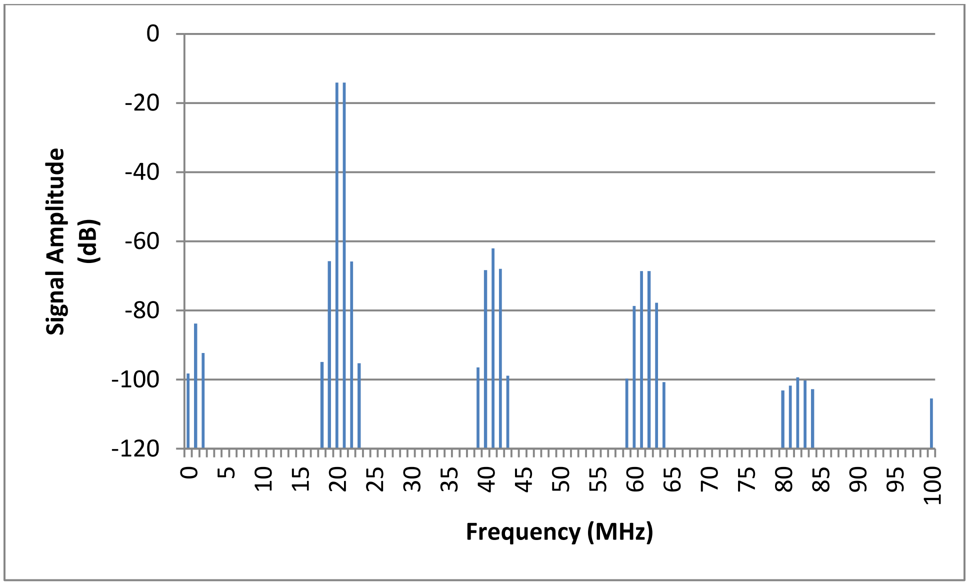

Fig. 33: The intermodulated distortion of the complete circuit.

The linearity of the entire circuit is demonstrated in figure 34. Similar to the test for the TIA a single ended input is provided. Each input has an amplitude of 2μA and they are at 20MHz and 21MHz. The SFDR of the system is 48dB, slightly below the design goal of 50dB.

. Two transient simulations with a single ended input with an amplitude of 4μA and frequency of 20MHz are shown in figures 34 and 35. Figure 34 shows the output response without any DC input offset. It shows both the positive and negative terminal and the difference between the two.

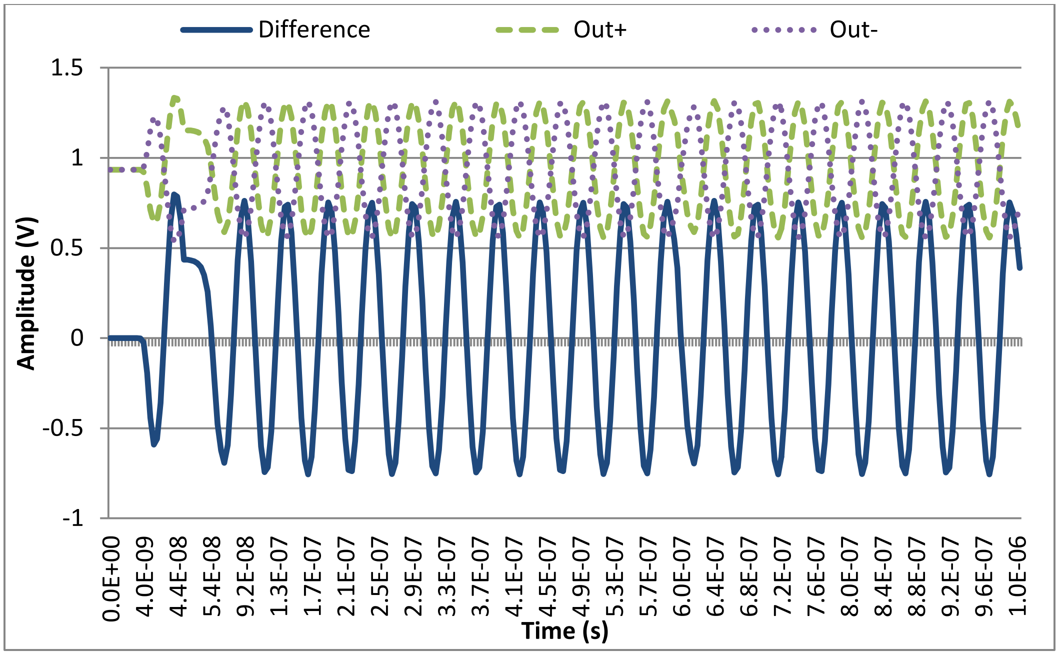

Fig. 34: Transient output simulation.

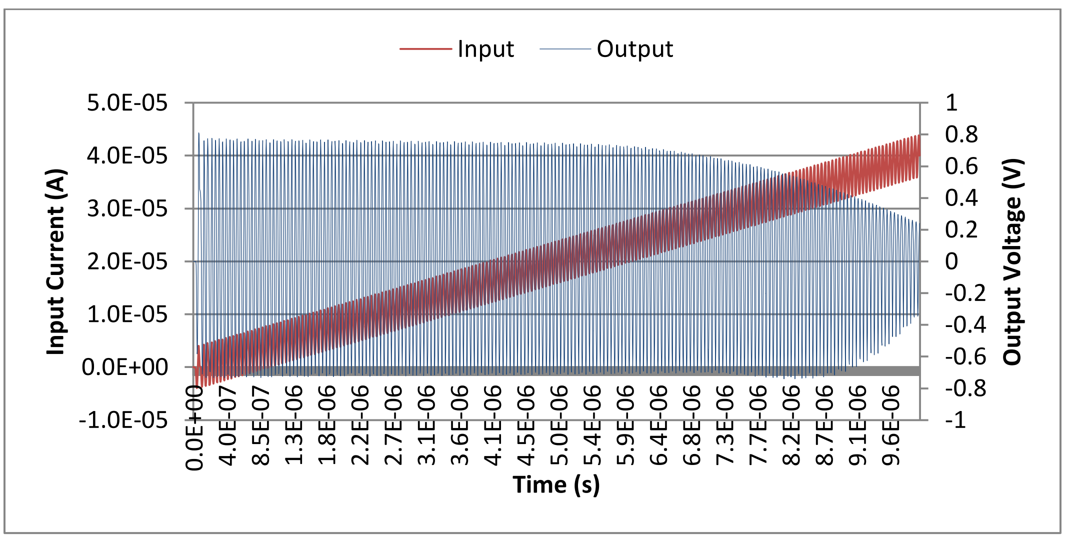

Fig. 35: Transient simulation with slow rising DC offset of 0A to 40µA.

Figure 35 shows the output while a slowly increasing DC offset is added the input. The input is composed of a current signal with a 4µA amplitude at 20MHz on top of a 0-40µA ramp over 10µs. Some output distortion shows up with an input offset of 30µA. This distortion could have been reduced by increasing the bias current of the OTA, but would have resulted in larger input referred noise. The noise contribution from the OTA is explained in section 3.7 and shows how the bias current and noise are directly proportional.

Figure 36 shows the output current of the OTA with the same input used for figure 35. The purpose of this graph is show how any DC offset at the input of the TIA is compensated for by the feedback OTA. The single ended to differential conversion is shown as each output of the OTA sinks half of the offset current. A complete summary of the system performance and design specifications is shown in table 6.

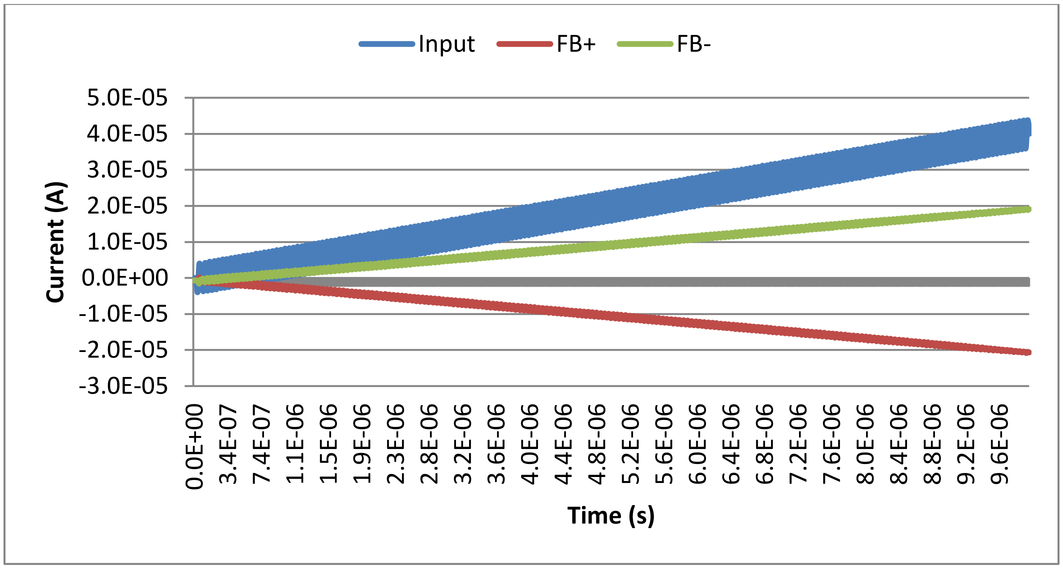

Fig. 36: Transient simulation showing input DC offest and feedback current through the OTA.

Table 7: Summary of the system performance and design specifications.

Parameter	Specification	Simulated Value

Transimpedance Gain	210kΩ (106.4dBΩ)	200kΩ (106dBΩ)
Parasitic Input Capacitance	0.8pF	0.8pF
Input Dynamic Range	4nA to 4µA	48dB SFDR with 4µA input
Output Dynamic Range	1mV to 1V	$1.5V_{p\text{-}p}$
Input Referred Noise	$0.35 pA/\sqrt{Hz}$	$11\, pA/\sqrt{Hz}$
Bandwidth	15MHz to 35MHz	5MHz to 45MHz
DC Offset Cancellation	0 to 40µA	0 to 40µA

4.6 CONCLUSION

The primary design goals of a high gain, wide band amplifier with input offset cancellation were met. The Cherry-Hooper design allows for a high gain, wide bandwidth design that is completely decoupled from the input parasitic capacitance. This makes a suitable amplifier for any large area photodiode that has large parasitic capacitance in the picofarad to tens of picofarad range. Also, because the response of the amplifier is independent of the parasitic capacitance value it can dropped into any system regardless of the photodiode.

Moving forward with this project will be designing an amplifier for use with a specific photodiode in a laser vibrometer system. It became clear as the program progressed that an amplifier that can be used with a wide range of diodes will not have the noise performance required by a laser vibrometer system. The analysis provided shows that neither the Cherry-Hooper TIA topology nor servo loop feed should be used for a low noise design.

REFERENCES

[1] C. Hermans and M. Steyaert, “Broadband Opto-Electrical Receivers in Standard CMOS”, pp.61-103, Springer, 2007

[2] W.M.C Sansen, “Analog Design Essentials”, Springer, 2006

[3] R. J. Baker, “CMOS Circuit Design, Layout, and Simulation”, John Wiley & Sons, Inc., 2008

[4] S. M. Park, “1.25-Gb/s regulated cascode CMOS transimpedance amplifier for Gigabit Ethernet applicatinos”, IEEE Journal of Solid-State Circuits, pp. 112, Jan. 1, 2004

[5] Holdenried, “Analysis and design of HBT Cherry Hooper amplifier with emitter follower feedback for optical communication”

[6] W.-Z. Chen, Y.-L. Cheng, D.-S. Lin, “A 1.8V 10Gb/s fully integrated CMOS optical receiver analog front-end”, IEE Journal of Solid-State Circuits, pp. 1388-1396, June 2005

[7] H.-Y. Hwang, J.-C. Chien, T.-Y. Chen, L.-H. Lu, “A CMOS tunable transimpedance amplifier,” IEEE Microwave Wireless Components Letters, pp. 693-695, Dec. 2006

[8] J. Lee, S.-J. Song, S.M. Park, C.-M. Nam, Y.-S. Kwon, H.-J. Yoo, “A multichip on oxide of 1Gb/s 80dB fully-differential CMOS transimpedance amplifier for optical interconnect applications,” IEEE International Solid-State Circuits Conference, Feb. 2002

[9] R.Y. Chen, T.-S. Hung, C.-Y. Hung, “A CMOS infrared wireless optical receiver front-end with a variable-gain fully-differential transimpedance amplifier,” IEEE Transactions on Consumer Electronics, pp.424-429, May 2005

[10] S. Goswami, J. Silver, T. Copani, W. Chen, H. J. Barnaby, B. Vermeire, S. Kiaei, “A 14mW 5Gb/s CMOS TIA with gain-reuse regulated cascade compensation for parallel optical interconnects,” IEEE International Solid-State Circuits Conference, Feb. 2009

[11] M. Fortunato, “A new filter topology for analog high-pass filters”, TI Analog Applications Journal, pp. 18-24, 3Q, 2008

[12] Bespalko, R (2007) *Transimpedance Amplifier Design using 0.18μm CMOS Technology*, unpublished thesis (M.S), Queen’s University

[13] Chandrashekar, K (2007) *Wide Bandwidth Transimpedance Amplifier using Modified Cherry Hooper Amplifier*, unpublished thesis (M.S), Arizona State University

[14] Abe, T. and Sugimoto, T, “Extremely shallow underground imagining using scanning laser Doppler vibrometer”, Japanese Journal of Applied Physics, Vol. 28, Issue 7, 2009